Summer 8-19-2016

Role of DDR1 in Pancreatic Cancer

Huocong Huang
University of Nebraska Medical Center

ROLE OF DDR1 IN PANCREATIC CANCER

by

Huocong Huang

A DISSERTATION

Presented to the Faculty of

The University of Nebraska Graduate College

in Partial Fulfillment of the Requirements

for the Degree of Doctor of Philosophy

Biochemistry & Molecular Biology

Graduate Program

Under the Supervision of Professor Keith R. Johnson

University of Nebraska Medical Center

Omaha, Nebraska

July, 2016

Supervisory Committee:

James K. Wahl, Ph.D.

Parmender Mehta, Ph.D.

Joyce Solheim, Ph.D

ROLE OF DDR1 IN PANCREATIC CANCER

Huocong Huang, B.Med., Ph.D.

University of Nebraska Medical Center, 2016

Supervisor: Keith R. Johnson, Ph.D.

Pancreatic ductal adenocarcinomas are highly malignant cancers, characterized by extensive invasion into surrounding tissues, metastasis to distant organs at a very early stage, and a limited response to therapy. One of the main features of pancreatic ductal adenocarcinomas is desmoplasia, which leads to extensive deposition of collagen I. We have demonstrated that collagen I can induce epithelial-mesenchymal transition (EMT) in pancreatic cancer cells. A hallmark of EMT is an increase in the expression of a mesenchymal cadherin, N-cadherin. Our previous studies have shown that up-regulation of N-cadherin can promote tumor cell invasion and that collagen I-induced EMT is through two collagen receptors α2β1 integrin and discoidin domain receptor 1 (DDR1). DDR1 is a receptor tyrosine kinase widely expressed during embryonic development and in many adult tissues. It is also highly expressed in many different cancers. However, the role of DDR1 in pancreatic cancer is largely unknown. In the collagen I-induced up-regulation of N-cadherin signaling pathway, we have shown that Proline-rich tyrosine kinase 2 (Pyk2) is downstream of DDR1. In this study, we found that isoform b of DDR1 is responsible for collagen I-induced up-regulation of N-cadherin and that it is Tyrosine513 of DDR1b that is involved. Knocking down Shc1, which binds to Tyrosine513 on DDR1b, eliminates N-cadherin up-regulation. We also found that the signaling is mediated by the interaction between the central domain of Shc1 and the proline-rich region of Pyk2. Taken together, these data illustrate that DDR1b, and not DDR1a, specifically mediates collagen I-induced N-cadherin up-regulation and that Shc1 is involved in this process.

TABLE OF CONTENTS

LIST OF FIGURES

Chapter V

Chapter VI

Chapter VII

LIST OF ABBREVIATIONS

α SMA	α-smooth muscle actin
BMP	bone morphogenetic protein
CH1 region	collagen homology 1 region
CrkII	CT10-regulated kinase II
Csk	c-src tyrosine kinase
CTCs	circulating tumor cells
DDR1	discoidin domain receptor 1
ECM	extracellular matrix
EGF	epidermal growth factor
EMT	epithelial-to-mesenchymal transition
EST	expressed sequence tag
FAK	Focal adhesion kinase
FAT domain	focal adhesion targeting domain
FERM domain	protein 4.1, ezrin, radixin, moesin domain
FGF	fibroblast growth factor
FGFR	fibroblast growth factor receptor
Grb2	growth factor receptor-bound protein 2
JM domain	juxtamembrane domain
LEF-1	lymphoid enhancer-binding factor-1
mAb	monoclonal antibody
MBP	maltose binding protein
MKK	MAPK kinase
MLK	mixed lineage kinases
MMTV	mouse mammary tumor virus
Nck1	non-catalytic region of tyrosine kinase adaptor protein 1

NHERF	Na^+/H^+ exchanger regulatory factor
pAb	polyclonal antibody
PCR	polymerase chain reaction
PDAC	pancreatic ductal adenocarcinoma
PTB domain	phosphotyrosine binding domain
PR	proline rich motif
Pyk2	Proline-rich tyrosine kinase 2
p130CAS	p130 Crk-associated substrate
RIPA buffer	Radio-Immunoprecipitation Assay buffer
RTK	receptor tyrosine kinase
RT-PCR	reverse transcription polymerase chain reaction
Shc1	Src homology and collagen homology 1
SH2 domain	Src Homology 2 domain
TCF	T-cell factor
TGFβ	transforming growth factor–β
TM domain	transmembrane domain
TNE buffer	Tris/NP40/EDTA buffer
YAP1	yes-associated protein 1

DEDICATION

First of all, I would like to thank my supervisor, Dr. Keith R. Johnson, for his mentorship through my graduate training. Despite my lack of experiences, he took me in his laboratory and taught me from the very basics of scientific research and critical thinking. I have been constantly inspired and encouraged by his strong enthusiasm in research and knowledge. Throughout the years, I have learned what real science is from him. I am thankful for the resources he provided to pursue my studies, at the same time, discussing with me and trying to solve every single problem during my research. He is not only a mentor but a great man full of wisdom and knowledge. I owe every bit of my accomplishments to his mentorship and thank him again for giving the priceless ticket to enter the world of science. Also, I am fortunate to have a very supportive, knowledgeable and experienced supervisory committee. I thank the supervisory committee members, Dr. James K. Wahl, Dr. Parmender Mehta, and Dr. Joyce Solheim, for their insightful suggestions during every committee meeting. I would like to thank the past and present members of the laboratory. I would like to thank Dr. Margaret J. Wheelock, for starting this lab together with Dr. Johnson, and having contributed so much to the field. I would like to thank Dr. Yasushi Shintani, who started the project and has done a lot of previous work. I would like to thank Robert A. Svoboda, who has made so many constructs in my studies. I would like to thank Jintana Saowapa, who has been a great friend in the lab, and has helped me in all kinds of aspects. I appreciate the delicious food she has made too. None of the achievements would be possible without the support from other members of the laboratory. I am especially grateful for the love from my family. My father Jianbin Huang, my mother Xueyi Huang, my sister Xiaoyu Huang, and my girlfriend Luyu Xie, they are my greatest spiritual support throughout the years. Without their love and care, I wouldn't have gone so far. Their faith in me enables me to become who I am today.

Last but not least, I would also like to thank the Biochemistry and Molecular Biology Department and acknowledge the funding support from Graduate Studies Research Assistantship.

Chapter I

Introduction

1. PANCREATIC CANCER AND STROMA

Pancreatic ductal adenocarcinoma (PDAC) is currently the fourth leading cause of cancer-related mortality in the US, with a five-year survival rate of less than 6% (American Cancer Society, 2013). Despite progress made in cancer biology and the development of various cancer therapeutic strategies, the prognosis of PDAC still remains very poor. The unfortunate prognosis of this cancer is mainly due to the malignant behavior of its tumors. Extensive local invasion and early systemic dissemination are characteristics of pancreatic cancer. About 80% of patients already have regional or distant metastases when they are diagnosed with the disease (1). Only 10-15% of patients with advanced and metastatic disease have the chance to go through surgical resection. But regardless of surgery, most patients still relapse (2). Moreover, there remains no effective therapy available to treat this aggressive tumor. For the past two decades, patients have been treated with the nucleoside analog gemcitabine as the standard chemotherapy, which results in increasing median survival by only five weeks (3). More recently FOLFIRINOX (oxaliplatin, irinotecan, 5-fluorouracil, and leucovorin), although it has increased toxicity, improved median survival by about four months more in patients who can tolerate it compared to gemcitabine (4), however, this is still very short survival among all the cancers.

PDAC is characterized by its unique microenvironment formed by a very dense stroma, which plays a complex role in tumor progression (Figure 1). PDAC is one of the most stroma-rich cancers and the stroma can comprise as much as 90% of the total tumor volume (5, 6). It consists of a variety of cellular components including proliferating myofibroblasts (pancreatic stellate cells), macrophages, mast cells, lymphocytes, and plasma cells, and extensive extracellular matrix including type I collagen, proteoglycans, fibronectin and hyaluronic acid.

Figure 1. Microenvironment of PDAC is formed by a very dense stroma.

Masson's trichrome staining was performed in primary pancreatic cancer tissues. Tissues were obtained from Rapid Autopsy Program at the University of Nebraska Medical Center. Cytoplasm is stained red whereas collagen displays blue coloration.

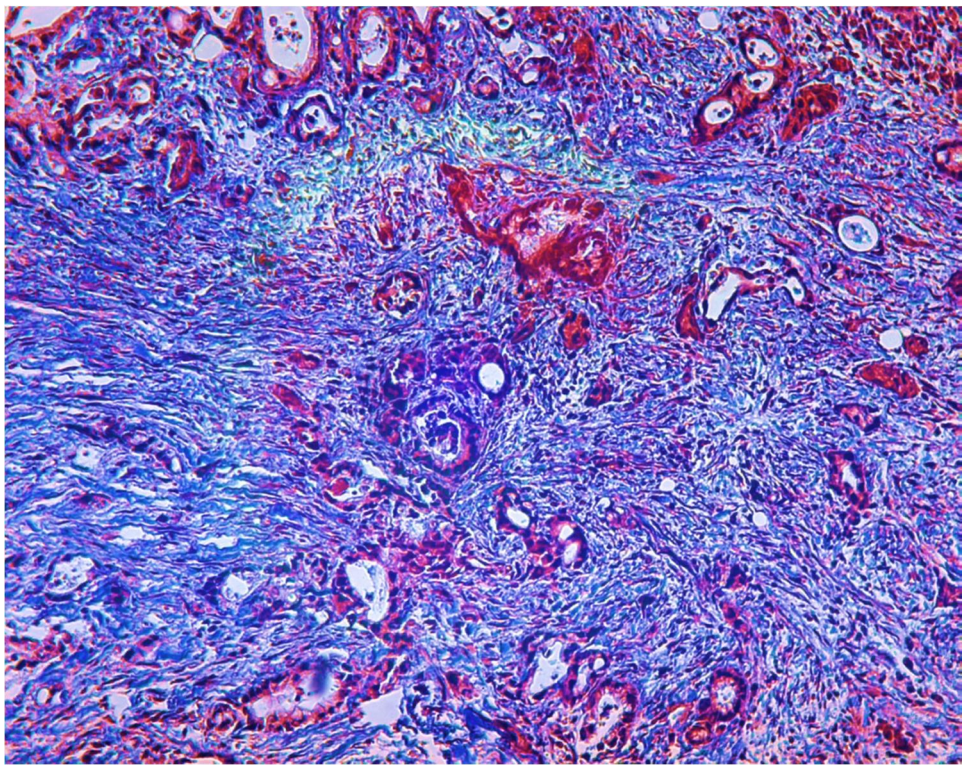

The stroma has many direct or indirect effects on disease progression. For example, *in vitro* studies showed that pancreatic stellate cells, which are the predominant fibroblasts present in the PDAC stroma, can increase proliferation, migration and invasiveness of pancreatic cancer cells, and orthotopic mouse models with pancreatic stellate cells and pancreatic cancer cells co-injection showed more aggressive and metastatic tumor formation (7, 8). During pancreatitis or PDAC, pancreatic stellate cells become activated. They acquire a myofibroblast-like phenotype, and express the fibroblast activation marker α-smooth muscle actin (αSMA) (9). These activated pancreatic stellate cells secrete excessive amounts of extracellular matrix (ECM) causing desmoplasia and a fibrotic microenvironment (5). Pancreatic stellate cells also secrete different matrix metalloproteinases, which play an important role in ECM turnover and tissue architecture (10). Although many studies reported that pancreatic stellate cells promote PDAC, it has to be mentioned that several studies recently (11-13) showed that depleting the pancreatic stellate cells accelerates tumorigenesis and results in a more aggressive cancer phenotype with high invasiveness, increased hypoxia, and reduced survival. These results indicate that pancreatic stellate cells may restrain tumor growth and highlight the complexity of the PDAC stroma and the need for further understanding of each stromal component and the complex signaling interactions in the PDAC microenvironment. Besides pancreatic stellate cells, many immune cells also contribute to tumor progression by restricting immune surveillance and creating an inflammatory response that supports tumorigenesis (14). During the early stage of tumor formation, immunosuppressive regulatory T cells and myeloid cells are recruited to the tumor stroma by the cytokine granulocyte–macrophage colony-stimulating factor produced by tumor cells (15), moreover, tumor-associated macrophages are also recruited to the microenvironment (16). All of these will eventually lead to suppression of antitumor immunity. Besides cellular components, acellular components within the stroma can also contribute to tumor progression indirectly. The dense fibrous stroma will create a hypovascular environment, reducing blood flow and increasing interstitial pressure (17). This will impair drug delivery, which is one of the major reasons of the

extremely poor prognosis of the disease and its resistance to systemic therapies (5, 18). It has been reported that in an orthotopic pancreatic cancer mouse model with little stromal formation, the intracellular metabolite of gemcitabine was detected at a high concentration and it exerted optimal anti-tumor effects (19). In contrast, in Pdx1-Cre; K-Ras$^{+/LSLG12D}$; p53$^{R172H/+}$ (KPC) mice (a genetically engineered mouse model of pancreatic adenocarcinoma), which are characterized by pronounced desmoplastic reactions, the intracellular metabolite of gemcitabine was hardly detectable and the drug had little effect on tumors (19).

The formation of stroma within PDAC has been attributed to signaling between cancer and its microenvironment involving paracrine and autocrine signaling pathways. Many signaling pathways have been reported to be potent modulators of the stroma. As potential therapeutic strategies, many clinical trials are undergoing trying to target these signaling pathways. For example, the Sonic hedgehog signaling pathway has been shown to mediate desmoplasia (19), so chemical inhibitors have been developed targeting this signaling pathway and brought to clinical trials (20), including GDC-0449 (Genentech/Curis) and IPI-926 (Infinity Pharmaceuticals), with which there are six clinical trials going on in the United States. Another such signaling pathway is the TGF-beta pathway (21, 22). A randomized, active-controlled study in pancreatic cancer patients is in preparation with the antisense oligonucleotide trabedersen (AP 12009) inhibiting TGF-beta2 synthesis (23). Besides targeting the signaling pathways that contribute to desmoplasia, the abundant ECM can also be a potential target. As it was mentioned before, ECM can increase interstitial fluid pressure and promote hypovascularity, which impairs perfusion and cause inefficient drug delivery. Pegylated hyaluronidase (PEGPH20), a recombinant hyaluronidase that can degrade hyaluronic acid, a major component of the pancreatic cancer ECM, has been shown to decrease interstitial fluid pressure in the stroma, increase vascularity, and improve drug delivery in genetically engineered mouse models of PDAC (17). A recent clinical

trial with PEGPH20 in advanced PDAC patients has shown some therapeutic benefit, especially in the tumors with high hyaluronic acid (24).

Over the past decades, it has been increasingly evident that PDAC and its stroma have very dynamic interactions, and these interactions play a critical role in tumor initiation, progression and metastasis. Much more work has to been done to understand the complex interactions and the signaling pathways involved before we can develop novel therapeutic targets or overcome the problems of the existing therapies for pancreatic cancer.

2. EMT AND CANCER

During early metazoan embryogenesis, a process called EMT happens. EMT enables an epithelial cell to convert into a mesenchymal cell with the ability to migrate and invade adjacent tissues. The hallmarks of the EMT include loss of cell-cell junctions, loss of apical-basal cell polarity, and acquisition of migratory and invasive properties (25). Through changing their phenotype and taking on mesenchymal characteristics, cells can migrate long distances and move into the interior of the embryo, and eventually settle, proliferate, and differentiate into different organs (25, 26). Cells disrupt cell-cell adhesion contacts within the primitive epithelial layer and ingress. For example, the ingression of mesendodermal precursors at the primitive streak in amniotes and the delamination of the neural crest all involve EMT. Moreover, all vertebrate adult tissues originate from cells that underwent at least one EMT.

Like embryonic tissues, EMT also happens in many types of cancer including PDAC (27). Cancer cells undergo EMT and convert into mesenchymal cells with migratory and invasive properties in order to escape from primary carcinomas (25). The application of sophisticated imaging techniques in mouse and rat cancer models and the characterization of circulating tumor cells (CTCs) from patients have shown cancer cells with EMT signatures (28-30). These provided evidence that EMT occurs during dissemination of metastatic cells from a primary tumor. Cancer

can be initiated and propagated by the certain group of cells that go through EMT and gain stem cell properties (31). Even though there are many similarities between the EMT during development and the one in cancer, there are also obvious differences. So EMT can be classified into three different types (32). Type 1 refers to developmental EMT, type 2 refers to the EMT happening during wound healing and tissue regeneration, and type 3 refers to the EMT in cancer. Tumor cells undergo type 3 EMT, which is different from the other two types, that often involves intravasation of delaminated cells into lymphatic and blood vessels and then extravasation. However, cells that have not undergone EMT are not able to intravasate into blood vessels to develop blood-borne metastasis (33). Although EMT often means loss of epithelial traits and gain of mesenchymal features, it is important to bear in mind that EMT is not necessarily an "all-or-nothing" or "black-or-white" transition. Partial EMT also happens, in which cells have both epithelial and mesenchymal traits (34, 35).

EMT can be triggered by many different extracellular signals in cancer. For example, members of transforming growth factor–β (TGFβ)/bone morphogenetic protein (BMP) family, Wnt, Notch, epidermal growth factor (EGF), and fibroblast growth factor (FGF) have been shown to induce EMT very potently (25). Different extracellular signals converge in cancer cells and further activate one or several EMT transcription factors including Snail, Twist and Zeb, which repress the epithelial phenotype, enhance mesenchymal traits and cause a dramatic change in cell behavior by increasing the capability of migration and survival in adverse environments (36). Once the EMT transcription factors are activated, they can in turn increase the transcription of genes encoding proteins in the same signaling pathways in order to generate positive regulatory loops that help maintain the mesenchymal phenotype in cancer cells (37).

EMT has been shown to be associated with multidrug resistance and tumor relapse after chemotherapy (38, 39). Cells undergone EMT gain stem cell–like properties and resistance to cell death (40), so it is important that besides classical cytotoxic chemotherapy, we also need to

develop new therapeutic strategies to target the EMT process or cells that have undergone EMT, in order to prevent cancer from recurring. To target EMT, we can inhibit the signaling pathways that induce EMT, including TGFβ, Wnt, Notch, EGF, and FGF signaling pathways, as mentioned earlier. Moreover, we should combat cancer cells that have already undergone EMT and gained stem-like properties. A combination of classical chemotherapy with drugs targeting EMT simultaneously may be a good strategy for cancer treatment. As mentioned in the earlier section, the tumor microenvironment is very important in pancreatic cancer progression, and our lab found that PDAC stroma can also induce EMT in pancreatic cancer cells (41). Therefore, therapeutic strategies should also consider targeting the stroma as well as the interaction between stroma and pancreatic cancer cells.

3. CADHERINS AND CANCER

One of the hallmarks of the EMT is loss of cell-cell junctions. Epithelial cell-cell junctions help maintain tissue integrity and cell polarity. The junctional complex includes tight junctions, adherens junctions and desmosomes. The adherens junctions play a very important role in regulating the activity of the whole junctional complex, and they are formed by proteins called cadherins. Cadherins are transmembrane glycoproteins that mediate cell-cell adhesion in a Ca^{2+}-dependent manner (42). They mediate cell-cell adhesion through their extracellular domains and connect to the actin cytoskeleton by associating with catenins through their cytosolic domain. Classical cadherins include E-cadherin (which is expressed in epithelial cells), N-cadherin (in neural tissue, muscle and fibroblasts), R-cadherin (in the forebrain and bone), and P-cadherin (in the basal layer of stratified epithelia) (43). Classical cadherins, which consist of an adhesive extracellular domain with five external cadherin (EC) repeats, EC1-EC5, can be divided into two subtypes, type I and type II. Type I cadherins, which include E-cadherin, N-cadherin, R-cadherin and P-cadherin, are different from type II cadherins in that they have a highly conserved His-Ala-Val (HAV) tripeptide within the most distal external cadherin repeat (EC1), which can mediate

homophilic adhesion (44). Synthetic peptides containing the HAV sequence can inhibit cadherin-based compaction. Studies have shown that short cyclic HAV peptides such as ADH-1 (N-Ac-CHAVC-NH2) can inhibit N-cadherin function (45). Besides the HAV sequence, it has also been reported that a conserved tryptophan residue within EC1 is required for trans-cadherin binding (46). EC2, although it does not mediate cell-cell adhesion directly, has been reported to form the "minimal essential unit" together with EC1 and is responsible for homophilic adhesion activity (47). EC3-5 are also important for cell adhesion, but they may have some other roles also. Our lab found that a 69-amino acid portion of EC4 of N-cadherin can promote EMT in squamous epithelial cells and increase cell motility (48). Other groups reported that EC4 of N-cadherin interacts with the fibroblast growth factor receptor (FGFR), forming a complex that can facilitate cell motility, invasion, and metastasis (49, 50).

The cytoplasmic domain of classic cadherins is highly conserved and can interact with many cytosolic proteins. This domain can be associated with many catenin family members, including alpha-catenin, beta-catenin and p120 catenin (51, 52), and form a cadherin-catenin complex. p120 catenin binds to the juxtamembrane region of cadherins and stabilizes cadherins by masking an endocytic signal conserved in classical cadherins (53, 54). It can also regulate the actin cytoskeleton through Rho GTPases (55, 56). Beta-catenin is another catenin family member that binds to cadherins. Beta-catenin has also been identified as a nuclear trancriptional co-activator for the lymphoid enhancer-binding factor-1 (LEF-1)/T-cell factor (TCF) family of transcription factors, and it plays a very important role in the Wnt signaling pathways (57, 58), and E-cadherin binding can prevent beta-catenin nuclear localization and beta-catenin/LEF-1-mediated transactivation (51). Moreover, alpha-catenin, also associated with cadherins, has been reported to interact with yes-associated protein 1 (YAP1) and prevent YAP1 nuclear localization (59, 60). Therefore, besides mediating cell-cell adhesion, cadherins can also modulate many different signaling pathways through their binding partners.

Adherens junctions will be disrupted when cells undergo EMT, and a process called cadherin switching often happens (61). Cancer cells, which are originally epithelial cells, will switch from expressing E-cadherin, the epithelial type of cadherins, to expressing N-cadherin, the mesenchymal type. However, in some situations, E-cadherin expression levels do not change significantly, while N-cadherin expression levels are up-regulated. In some cases, instead of turning on N-cadherin, some other cadherins will be up-regulated, including R-cadherin, cadherin 11, T-cadherin and even P-cadherin. The expression of these "inappropriate cadherins" will change the behavior of the cancer cells so a certain population of cells can gain the ability to leave the site of the primary tumor and metastasize.

Many groups, including ours, have shown that N-cadherin increases motility in cancer cells regardless of E-cadherin expression (62, 63). As it was mentioned earlier, we found that EC4 of N-cadherin can promote EMT and increase cell motility in cancer. Many studies have suggested that N-cadherin is involved in fibroblast growth factor signaling (49, 64, 65). Moreover, we have also shown that the scaffolding molecule Na^+/H^+ exchanger regulatory factor (NHERF) links the N-cadherin/beta-catenin complex to the platelet-derived growth factor receptor to modulate the actin cytoskeleton and regulate cell motility (66). Therefore, when tumor cells up-regulate N-cadherin expression, they also gain the ability to activate many growth factor receptor signaling pathways to promote cell growth and metastasis. We have generated transgenic mice that expressed N-cadherin under control of the mouse mammary tumor virus (MMTV) promoter, and found that expression of N-cadherin alone in the mouse mammary glands does not initiate tumors (67). Moreover, even when we crossed the mice with the *neu* oncogene transgenic mice which can develop focal mammary tumors, there was no difference between the mice expressing *neu* alone and the ones expressing both *neu* and N-cadherin regarding aggressiveness of the tumors (67). However, another group crossed the MMTV-N-cadherin mice with mice expressing polyoma virus middle T antigen in the mammary epithelium, and they found that N-cadherin can

increase tumor metastasis (68). Therefore, role of N-cadherin in tumor progression might be context dependent. Our lab used orthotopic mouse models to study role of N-cadherin in pancreatic cancer (69). We injected mice with BxPC-3 human pancreatic cancer cells expressing endogenous N-cadherin, shRNA targeting N-cadherin, or exogenous N-cadherin (69). We found that N-cadherin promotes tumor metastasis in pancreatic cancer. Furthermore, we treated the orthotopic pancreatic cancer mouse models with short cyclic HAV peptides ADH-1 antagonizing N-cadherin (70). As a result, we found significant reductions in tumor growth and lung metastasis with ADH-1 treatment.

N-cadherin promotes cancer cells to become more aggressive by many different mechanisms. We need more studies to understand how N-cadherin influences cell behavior and how various signals, including signals from the tumor microenvironment, up-regulate the expression of N-cadherin. By better understanding more mechanisms in the pathways of cadherin switching, we may be able to develop some novel therapeutic strategies.

4. COLLAGEN-INDUCED EMT IN PANCREATIC CANCER

By using the pancreatic cancer cell line BxPC-3, our laboratory found that collagen I mediates up-regulation of N-cadherin and a cell scattering morphological change through cooperative signals from two collagen receptors, alpha2beta1 integrin and discoidin domain receptor 1 (DDR1) (41). In the previous study, knocking down beta1 integrin or DDR1 alone partially inhibited up-regulation of N-cadherin in BxPC-3 cells. However, knocking down both receptors resulted in complete inhibition of N-cadherin up-regulation. We found that when α2β1 integrin was activated, it further activated its downstream effector Focal adhesion kinase (FAK), while when DDR1 was activated, it activated another downstream effector Proline-rich tyrosine kinase 2 (Pyk2), which is very similar to FAK (Figure 2). Signals activated by collagen from both arms of the pathway fused to a scaffold protein called p130 Crk-associated substrate (p130CAS). Since

integrin or DDR1 binding to collagen each only initiated a partial response, the two partial signals are integrated by p130CAS to give a full response. Once p130CAS is activated, it activates the small GTPase Rap1. Then Rap1 activates the mixed lineage kinases (MLK) 3-MAPK kinase (MKK) 7-JNK1-cJun cascade, which promotes up-regulation of N-cadherin.

Figure 2. Model of the signaling pathway in BxPC-3 cells during collagen I-induced up-regulation of N-cadherin.

Collagen I mediates up-regulation of N-cadherin through cooperative signals from two collagen receptors alpha2beta1 integrin and DDR1.

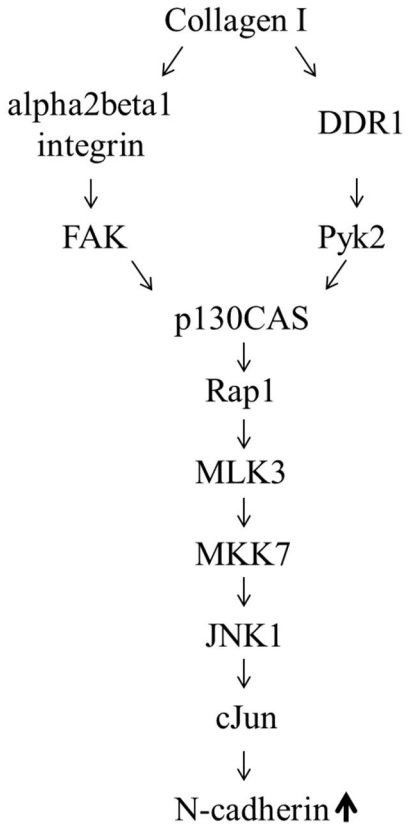
Collagen I
alpha2beta1 integrin
DDR1
FAK
Pyk2
p130CAS
Rap1
MLK3
MKK7
JNK1
cJun
N-cadherin

In this study, we have focused on the DDR1 arm of the signaling pathway and tried to identify the early steps in the signaling pathway that is initiated downstream of DDR1 when pancreatic cancer cells are exposed to collagen.

5. DISCOIDIN DOMAIN RECEPTORS

Discoidin domain receptors (DDRs) are type I transmembrane receptor tyrosine kinases (RTKs) characterized by an N-terminal extracellular discoidin domain containing a collagen binding site (71, 72) (Figure 3). There are two types of discoidin domain receptors, DDR1 and DDR2. DDR1 is expressed in epithelial cells, while DDR2 is expressed in mesenchymal cells (73). The collagen binding sites within the discoidin domains are highly conserved and DDRs can be activated by many different types of collagen (74-76). They all recognize the GVMGVO (O, hydroxyproline) motif within fibrillar collagens I–III and V. In addition, DDR1 and DDR2 also have their own binding specificity, with DDR1 only binding to collagen IV, and DDR2 only binding to collagen X. Since DDR binding sites on collagens are distinct from integrin binding sites, simultaneous activation of DDRs and integrins is possible, both of which contribute to up-regulation of N-cadherin in pancreatic cancer (41). Although the structures of DDRs are similar to many other RTKs, they are unique among RTKs because they have unusually slow kinetics of activation. After binding to collagen, DDRs can be autophosphorylated on tyrosine residues but requires hours to reach full activation, which can persist up to 18 hours.

The extracellular discoidin domain is followed by an extracellular (JM) membrane region, then a single transmembrane (TM) domain and an unusually large cytosolic JM domain which contains phosphorylatable tyrosines that may serve as docking sites for many other proteins. A catalytic kinase domain follows the cytosolic JM domain and at the very end comes a short C-terminal tail. There are five different isoforms of DDR1 (a-e) generated through alternatively splicing. The isoforms termed DDR1a and DDR1b are the most widely distributed, while the others are less

common (77). DDR1a lacks a 37-residue segment present in the cytosolic juxtamembrane region of DDR1b. This segment contains important phosphorylation sites. In the shorter DDR1a isoform, two tyrosines (Y513 and Y520) are missing. After phosphorylation, these Tyrosines are reported to bind Src homology and collagen homology 1 (Shc1) and c-src tyrosine kinase (Csk), respectively (71, 78, 79).

More and more studies indicate that DDR1 plays an important role in many cancers (80-84). However, we still don't understand the detailed molecular mechanisms of DDR1 signaling during cancer progression. Such understanding may result in inhibition of the signaling pathways and new therapeutic interventions for cancers including pancreatic ductal adenocarcinoma. Therefore, in this study, we tried to investigate how collagen initiates the signaling through DDR1 to up-regulate N-cadherin.

Figure 3. Structure of DDR1b.

DDR1 is a receptor tyrosine kinase characterized by an N-terminal extracellular discoidin domain. The discoidin domain is followed by an extracellular juxtamembrane region, then a single transmembrane domain and an unusually large cytosolic juxtamembrane domain which contains phosphorylatable tyrosines that may serve as docking sites for many other proteins. A catalytic kinase domain follows the cytosolic juxtamembrane domain and at the very end comes a short C-terminal tail. All the tyrosines within the cytoplasmic tail of DDR1b are shown (the yellow ones indicate they are conserved in human and mouse, and the blue one only exists in human). DDR1a lacks a 37-residue segment present in the cytosolic juxtamembrane region of DDR1b. This segment contains two important tyrosines (Y513 and Y520).

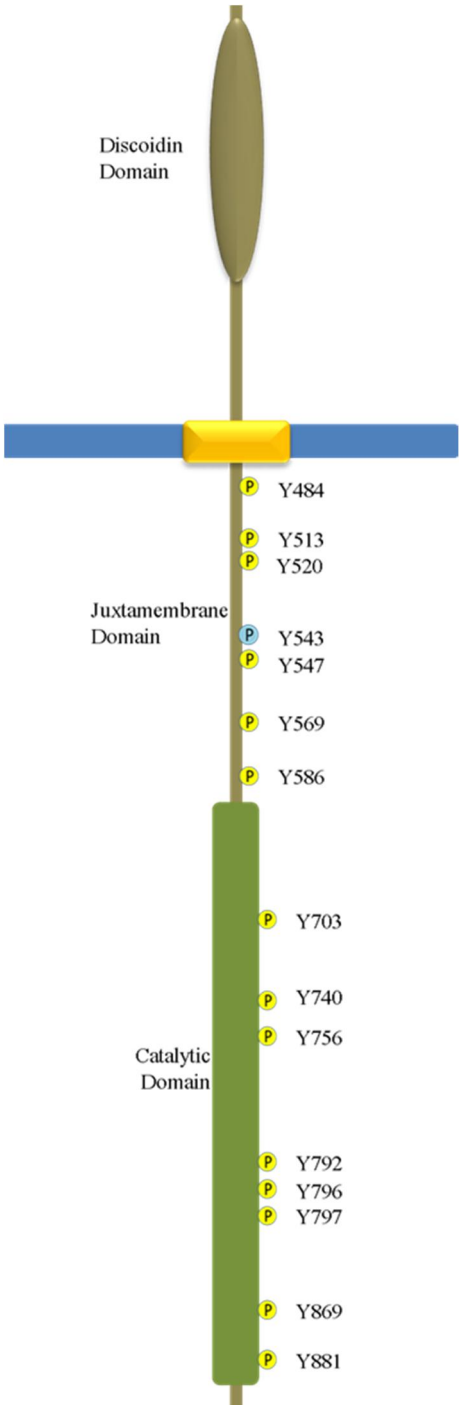
Discoidin
Domain
Y484
Y513
Y520
Juxtamembrane
Domain
Y543
Y547
Y569
Y586
Y703
Y740
Y756
Catalytic
Domain
Y792
Y796
Y797
Y869
Y881

Chapter II

Materials and Methods

1. REAGENTS AND ANTIBODIES

The mouse mAb against E-cadherin (HECD-1; hybridoma supernatant, western blot dilution 1:100) was a gift from Dr. M. Takeichi (RIKEN Center for Developmental Biology, Kobe, Japan) and the mouse mAb against N-cadherin (13A9; hybridoma supernatant, no dilution for immunohistochemistry, western blot dilution 1:100) has been previously described (85). Anti-tubulin mouse mAb E7 (western blot dilution 1:1000) (developed by Drs. M. McCutcheon and S. Carroll) was obtained from the Developmental Studies Hybridoma Bank (University of Iowa, IA, USA). Anti-DDR1 rabbit pAb (C-20; immunohistochemistry dilution 1:100, immunoprecipitation dilution 1:100, western blot dilution 1:1000) and anti-Shc1 mouse mAb (PG-797; immunoprecipitation dilution 1:100, western blot dilution 1:1000) were obtained from Santa Cruz Biotechnology, Inc. (Dallas, TX, USA). Anti-JNK1 mouse mAb (2C6; western blot dilution 1:1000), anti-JNK phosphospecific (Thr183/Tyr185) rabbit Ab (9251; western blot dilution 1:1000), anti-Pyk2 mouse mAb (5E2; western blot dilution 1:1000), anti-Pyk2 phosphospecific (Tyr402) rabbit Ab (3291; western blot dilution 1:1000), anti-Shc1 rabbit Ab (2432; western blot dilution 1:1000) and anti-HA rabbit mAb (C29F4; western blot dilution 1:1000) were obtained from Cell Signaling Technology (Danvers, MA, USA). Anti-phosphotyrosine mouse Ab (PY20; western blot dilution 1:1000) was obtained from BD Biosciences (San Jose, CA, USA). Anti-FLAG mouse mAb (M2; immunoprecipitation dilution 1:100) was obtained from Sigma-Aldrich Co. (St. Louis, MO, USA). Anti-HA mouse mAb (16B12; immunoprecipitation dilution 1:100) was obtained from Covance Research Products Inc. (Princeton, NJ, USA). Anti-GFP rabbit Ab (632376; western blot dilution 1:200) was obtained from Clontech Laboratories (Mountain View, CA, USA). Collagen I-coated dishes and rat tail collagen I were obtained from BD Biosciences. The synthesis of the DDR1-specific inhibitor 7rh has been described (86).

2. CULTURED CELLS

The identity of all the cell lines used in these experiments was verified by the University of Arizona Genetics Core (http://uagc.arl.arizona.edu/services/cell-line-authentication-human), and each cell line was shown to be free from mycoplasma using a PCR kit (PK-CA91-1048 from PromoCell (Heidelberg, Germany)). L3.6pl (87) was a gift from Drs. R. Singh and M. Ouellette (University of Nebraska Medical Center, Omaha, USA). PSN-1 was a gift from Dr. P. Tofilon (National Cancer Institute, Bethesda, USA). T3M-4 was a gift from Dr. T. Hollingsworth (University of Nebraska Medical Center, Omaha, USA). BxPC-3 was obtained from American Type Culture Collection. L3.6pl and T3M-4 were maintained in DMEM, and BxPC-3 and PSN-1 were maintained in RPMI 1640 containing 10% FBS respectively, in an atmosphere of 5% CO_2 at 37 °C.

3. DETERGENT EXTRACTION, SDS-PAGE, IMMUNOBLOT, AND IMMUNOPRECIPITATION

Monolayers of cultured cells were extracted with Tris/NP40/EDTA (TNE) buffer (10 mM Tris-HCl, pH 8.0, 0.5% Nonidet P-40, and 1 mM EDTA) for SDS-PAGE or immunoprecipitation as previously described (88). Protein was determined using a protein assay kit (Thermo Scientific (Waltham, MA, USA)). Antibodies were added to the indicated volume of cell extract and gently mixed overnight at 4°C. Anti-mouse or anti-rabbit IgG affinity gel (MP Biomedicals, Santa Ana, CA, USA) was washed with TNE buffer once. The cell extract-antibody mix was added to the IgG affinity gel and mixed at 4°C for 2 hours. Immune complexes were washed once with Radio-Immunoprecipitation Assay (RIPA) buffer (50 mM Tris-HCl, pH 8.0, 150 mM NaCl, 0.1% SDS, 0.5% sodium deoxycholate and 1% Nonidet P-40) and two times with TBST (10 mM Tris-HCl, pH 7.5, 150 mM NaCl, 0.05% Tween 20). After the final wash, the packed beads were resuspended in 50 µL of 2× Laemmli sample buffer, boiled for 5 min, and the proteins were resolved by SDS-PAGE. Proteins were electrophoretically transferred to nitrocellulose membranes and blocked in 5% nonfat dry milk or 5% bovine serum albumin in TBST for 1 hour.

Blocking solution was removed, and primary antibody in TBST was added followed by incubation for 1 h. Membranes were washed 15 min followed by 2×5 min in TBST. Membranes were incubated with horseradish peroxidase-conjugated anti-mouse or rabbit secondary antibody (Jackson ImmunoResearch Laboratories, West Grove, PA, USA) at 1:5,000 for 1 hour. The secondary antibody was removed by washing 15 min followed by 2×5 min in TBST. Immunoreactive bands were detected using SuperSignal West Pico substrate (Thermo Scientific).

4. CONSTRUCTS, TRANSFECTION, AND INFECTION

Phoenix cells (89) were transfected using TransIT-LT1 reagent (Mirus, Madison, WI, USA). Production of viral supernatants and infection of target cells have been described previously (90). 4 μg/mL puromycin, 200 μg/mL hygromycin or 1 mg/mL G418 was used for selection of the target cells.

The human DDR1a and DDR1b cDNAs were gifts from Dr. Teizo Yoshimura (National Cancer Institute, Bethesda, USA) (91). The DDR1a and DDR1b cDNAs were sequenced and shown to encode proteins identical to NP_001945.3 and NP_00054699.2, respectively. For stable expression in cells a monomeric EGFP (mEGFP, A206K) tag was added to the C-terminus of each isoform, eliminating the 3' UTRs. The tagged constructs were inserted into pLZRS-MS-Hygro or pLZRS-MS-Neo for stable expression. Gatekeeper mutants were generated by introducing a T664A mutation in DDR1a and a T701A in DDR1b using the QuikChange II Site-Directed Mutagenesis Kit (Agilent Technologies, Santa Clara, CA, USA). The primers for the gatekeeper mutants were a sense primer, 5'-CTCTGCATGATTGCTGACTACATGGAGAAC-3', and an antisense primer, 5'- GTTCTCCATGTAGTCAGCAATCATGCAGAG-3'. DDR1b Y513F, Y520F and Y513F/Y520F mutants were generated using QuikChange Lightning Multi Site-Directed Mutagenesis Kit (Agilent Technologies). The primers for these mutants were (sense oligos only), 5'-CAATCCAGCCTTCCGCCTCCTTC-3' for Y513F, and 5'-

CAATCCAGCCTTCCGCCTCCTTCTGGCCACTTTCGCCCGTCCC-3' for Y513F/Y520F. We obtained the single Y520F mutant when we used the Y513F/Y520F primer.

Human p66Shc1 pcDNA3.1His was purchased from Addgene (Plasmid #32574, Accession NM_001130040.1) (92). The human p52Shc1 cDNA was purchased from GE Dharmacon (Lafayette, CO, USA; Clone ID: 4541216, Accession BC014158.2). Mouse 2X HA p46Shc1 (AA 46-469 of NP_035498.2), mouse 2X HA p52Shc1 (NP_035498.2), mouse 3X FLAG p52Shc1 wild-type, R397K, R175Q, Y313F, Y239F/Y240F and Y239F/Y240F/Y313F mutants were gifts from Dr. P. Siegel (McGill University, Montreal, Canada) and were all inserted into pMSCV-Blast vectors (93). We moved human p66Shc1, human p52Shc1 and mouse p46Shc1 into pLZRS-MS-Neo for stable expression. All mouse p46Shc1 truncation mutants (T1 through T7) were PCR products made using mouse 2X HA p46Shc1 in pMSCV-Blast as a template. The primers used were the common sense primer 5'-CTCCTTCTCTAGGCGCCGG-3' and the antisense primers T1: 5'-GAATTCTCACCTGTCATGGGGGGTGAC-3', T2: 5'-GAATTCTCAGTGGAACCAGGGCTCCG-3', T3: 5'-GAATTCTCAAGCAGCCCCTTCCCGAAG-3', T4: 5'-GAATTCTCAGTCTAGATTCTGGATGTTG-3', T5: 5'-GAATTCTCAGACTTCATGGTCTCCTGC-3', T6: 5'-GAATTCTCAATGCTGCCCTATAGGC-3', T7: 5'-GAATTCTCAGGACATCTGGGCACTAGG-3'. Both human p46Shc1 truncation mutants T6 and T7 were PCR products made using human p52Shc1 cDNA as a template. The primers used were the common sense primer 5'-GCTAGCACCATGGGACCCGGGGTTTCC-3' and the antisense primers T6: 5'-GGTACCGAATTCTCAAGGCTGTCCTACAGGCAATG-3', T7: 5'-GGTACCGAATTCTCAGGGGGTCTGGGCATTGGG-3'. The PCR products were inserted into pCR2.1 TOPO vectors and tagged at their N-termini with 2X HA. Then the human 2X HA p46Shc1 T6 and T7 were moved into pMSCV-Blast vectors. All the truncation mutants as well as

each construct we generated via PCR that was used in the experiments described in this manuscript were completely sequenced and shown to encode the desired AA sequences with no unintended changes.

Rat Pyk2 (Accession NP_59124.2, C-terminally myc tagged) and the mutants Y402F and K457A in pcDNA3 were gifts from Dr. Lee Graves (University of North Carolina at Chapel Hill, Chapel Hill, USA) (94). The truncation mutants of rat Pyk2 (NP_59124.2) were gifts from Dr. Jean-Antoine Girault (Institut du Fer à Moulin, Inserm, Paris, France) and were tagged at their N-termini with EGFP (95). The mouse EST cDNA of shorter Pyk2 isoform was purchased from GE Dharmacon (Clone ID: 1429254, Accession AI153373) and we inserted it into pEGFP-C2 vector.

cDNA fragments encoding portions of rat Pyk2 and mouse p46Shc1 were cloned into pGST-Parallel or pMBP-Parallel vectors (96). The fusion proteins were expressed in Rosetta2 cells (Novagen; Madison, WI USA) and purified on glutathione agarose or cross-linked amylose beads.

The human FLAG-tagged CrkII was a gift from Dr. Bruce Mayer (University of Connecticut Health Center, Farmington, USA; Accession BC001718.1) (97). We inserted the tagged cDNA into pLZRS-MS-Neo. GST-Grb2 was purchased from Addgene (Plasmid #46442; Grb2 accession NM_002086.4) (98). We inserted the cDNA into pLZRS-MS-Neo. The human 3X HA-tagged Nck1 cDNA was a gift from Dr. Wei Li (University of Southern California, Los Angeles, USA; Accession NM_006153.3) (99).

The shRNA constructs were as follows: DDR1 (TRCN0000121082, Sigma), Shc1 (shShc1 991, TRCN0000332991; shShc1 997; TRCN0000295997; shShc1 208, TRCN0000040208; shShc1 434, TRCN0000010434, Sigma). All the shRNAs were in the vector pLKO.1-Puro. For a negative control, we used pLKO.1-puro carrying a sequence targeting EGFP (a gift from Dr. Angie Rizzino, University of Nebraska Medical Center, Omaha, USA).

5. CONVENTIONAL REVERSE TRANSCRIPTION (RT)-PCR

Total RNA was extracted with the RNeasy Plus Mini Kit (Qiagen; Alameda, CA USA) and analyzed by RT-PCR using a Titanium One-Step RT-PCR kit (Clontech). Primers used for PCR were the sense primer, 5'-GAGCTGACGGTTCACCTCTCTGTC-3', and the antisense primer, 5'-CAATGTCAGCCTCGGCATAATGG-3'. The conditions for PCR were as follows: 94°C for 45 s, 60°C for 30 s, and 72°C for 90 s for 15, 25 or 35 cycles. PCR products were analyzed by electrophoresis on 1.5% agarose gels.

6. IMMUNOHISTOCHEMISTRY

Tissue microarray slides were obtained from Rapid Autopsy Program at the University of Nebraska Medical Center (100). Slides were deparaffinized with xylene, rehydrated with an alcohol gradient and washed with water. Antigen retrieval was performed with an alkaline citrate buffer and microwave treatment. Peroxidase activity was quenched by 3% hydrogen peroxide. Slides were blocked with 5% bovine serum albumin and incubated with primary and secondary antibodies. 3, 3'-Diaminobenzidine substrate was added followed by hematoxylin counterstaining. Slides were evaluated and annotated by a pathologist (Dr. Audrey J. Lazenby). The score scale ranged from 0 to 3, with 0 being no staining or <10% cancer cells stained, 0.5 being faint to weak staining in >10% cancer cells, 1 being weak staining in >10% cancer cells, 1.5 being weak to moderate staining in >10% cancer cells, 2 being moderate staining in >10% cancer cells, 2.5 being moderate to strong staining in >10% cancer cells, 3 being strong staining in >10% cancer cells, and 3.5 being very strong staining in >10% cancer cells. Spearman correlation analysis was then performed.

7. CELL INVASION ASSAY

Cells (1.5×10^5) were plated in the upper chamber of BD BioCoat Matrigel Inserts (24-well plates, pore size = 8 μm; BD Biosciences). Culture medium containing 0.5% FBS was added to the upper chambers, and medium containing 10% FBS was added to the bottom chamber. When

it was used, 1NM-PP1 (Calbiochem; San Diego, CA USA) was added to both upper and bottom chambers. Cells were incubated on the membranes for 18 hours, and motility was quantified as described (101).

Chapter III

DDR1b is More Potent than DDR1a in Mediating Collagen I-induced Up-regulation of N-cadherin in Pancreatic Cancer Cells

First of all, we examined the expression of DDR1 and N-cadherin in tissues from human pancreatic cancer patients, comparing cancerous with uninvolved tissues (Figure 4). The immunohistochemistry showed that both DDR1 and N-cadherin are up-regulated in primary pancreatic cancer tissues as well as in liver metastases. Moreover, we performed correlation analysis in both primary and metastatic sites, and found that expression levels of DDR1 and N-cadherin in the cancerous tissues are highly correlated (Figure 4b).

We have shown that collagen I can activate DDR1 and induce the up-regulation of N-cadherin (41). As noted above, DDR1a and DDR1b are the two major isoforms of DDR1. We first determined which isoforms are expressed in several pancreatic cancer cell lines by performing RT-PCR with primers flanking the alternatively spliced exon to semi-quantitatively measure the mRNA levels of DDR1a and DDR1b. We found that both DDR1a and DDR1b are expressed in BxPC-3, T3M-4 and L3.6pl cells, and the expression levels of transcripts encoding DDR1a and DDR1b are similar (Figure 5). We then set out to test if both of them could mediate collagen I-induced up-regulation of N-cadherin. We used L3.6pl cells to dissect the details of the DDR1 signaling pathway because we found the response of these cells to collagen is primarily mediated by the DDR1 arm of the pathway.

We stably knocked down DDR1 in L3.6pl cells with a lentiviral shRNA targeting the 3'UTR. DDR1 knockdown cells as well as control cells were plated on collagen I-coated dishes (Figure 6). We found that after DDR1 knockdown, collagen I failed to induce N-cadherin up-regulation when compared to the control. We then introduced either DDR1a-mEGFP or DDR1b-mEGFP into the DDR1 knockdown cell lines (Figure 6). We found that up-regulation of N-cadherin in response to collagen I was fully rescued in cells expressing DDR1b but not in cells expressing DDR1a.

Figure 4. Expression of DDR1 and N-cadherin is correlated in human pancreatic cancer tissues.

(a) Immunohistochemical staining for DDR1 or N-cadherin was performed on uninvolved pancreatic tissues and primary pancreatic cancer tissues, as well as liver metastases. Two representative samples (Case 1 and Case 2) representing low DDR1/N-cadherin and high DDR1/N-cadherin expression, respectively, are shown. Cancerous lesions are indicated by red arrows. Original magnification, 400x. (b) Immunohistochemical staining for DDR1 or N-cadherin in uninvolved pancreatic tissues (n=5), primary pancreatic cancer tissues (n=10; labeled P on the graph) and liver metastases (n=30; labeled M on the graph) were scored and analyzed. P values reflect pairwise comparisons using Student's t-test. Spearman correlation analysis was performed with primary tumor tissues or liver metastases, r=0.85468, $p<0.01$ (primary tumor); r=0.8084, $p<0.001$ (metastasis).

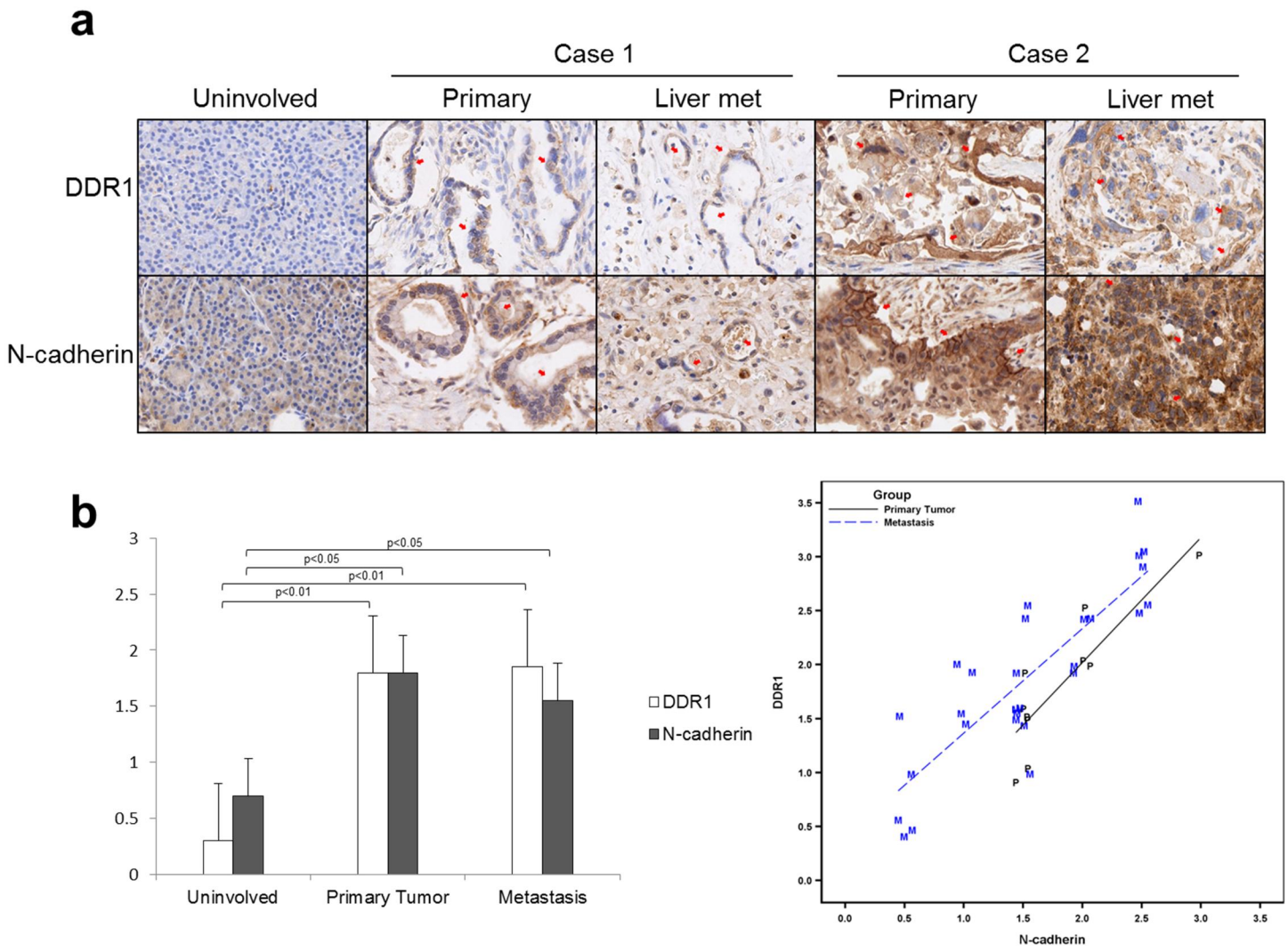
a
Case 1
Case 2
Uninvolved
Primary
Liver met
Primary
Liver met
DDR1
N-cadherin
b
p<0.05
p<0.05
p<0.01
p<0.01
3
2.5
2
1.5
1
0.5
0
Uninvolved
Primary Tumor
Metastasis
DDR1
N-cadherin
Group
Primary Tumor
Metastasis
DDR1
N-cadherin
0.0
0.5
1.0
1.5
2.0
2.5
3.0
3.5

Figure 5. Pancreatic cancer cells express both DDR1a and DDR1b.

RT-PCR was performed with primers flanking the alternatively spliced exon to semi-quantitatively measure the mRNA levels of DDR1a and DDR1b in pancreatic cancer cell lines BxPC-3, T3M-4, and L3.6pl. Human DDR1a and DDR1b cDNAs were used as templates to generate the markers (arrows).

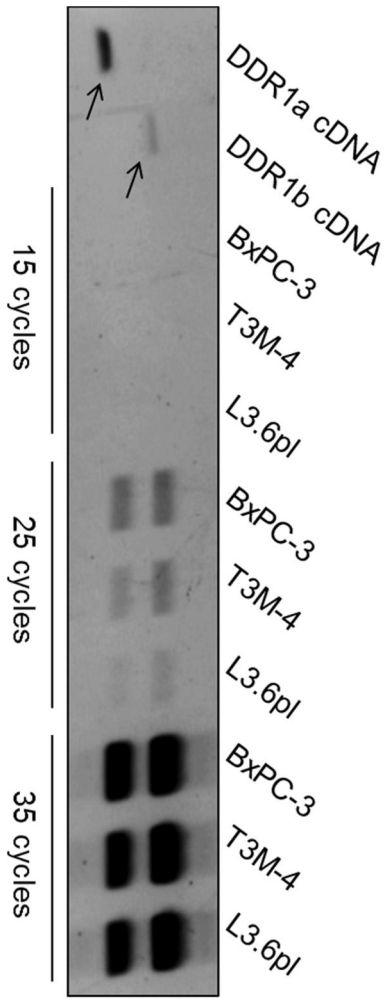
DDR1a cDNA
DDR1b cDNA
BxPC-3
T3M-4
L3.6pl
BxPC-3
T3M-4
L3.6pl
BxPC-3
T3M-4
L3.6pl
15 cycles
25 cycles
35 cycles

Figure 6. DDR1b is more potent than DDR1a in mediating collagen I-induced up-regulation of N-cadherin.

Parental L3.6pl cells and a number of derived cell lines were plated on tissue culture plastic (lanes 1-4, w/o col I) or collagen-coated plates for 18 hours (lanes 5-8, col I). Cell extracts were blotted with antibodies for DDR1, E-cadherin, N-cadherin and β-tubulin as a loading control. L3.6pl cells were stably infected with constructs expressing shRNA to EGFP (lanes 1&5) or shRNA targeting DDR1 (lanes 2-4, 6-8). We then introduced either DDR1a-mEGFP (lanes 3&7) or DDR1b-mEGFP (lanes 4&8) into the knockdown cells. The DDR1 cDNAs were fused to monomeric EGFP (mEGFP) to shift the molecular weight in order to verify that endogenous DDR1 was stably knocked down in cells expressing the isoform-specific cDNAs. In some experiments, as seen here in lanes 1&5, the level of endogenous DDR1 was down-regulated in cells plated for 18 hours on collagen, perhaps due to endocytosis or proteolysis of the receptor following exposure to its ligand. The asterisk marks a non-specific band recognized by the DDR1 antiserum.

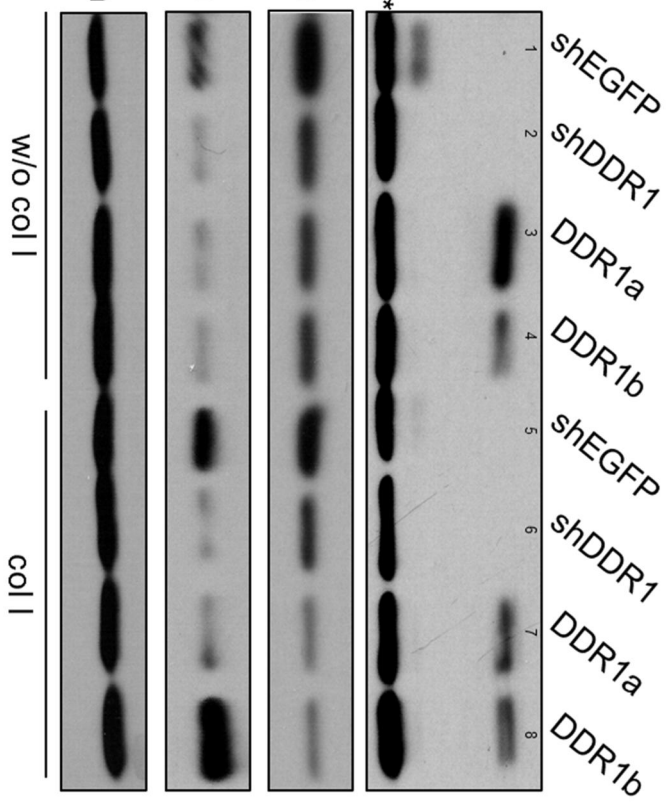
shEGFP
shDDR1
DDR1a
DDR1b
shEGFP
shDDR1
DDR1a
DDR1b
1
2
3
4
5
6
7
8
DDR1
*
E-cadherin
N-cadherin
β-tubulin
w/o col I
col I

Protein kinases such as DDR1a and DDR1b have residues termed gatekeepers that limit access to the ATP-binding pocket (102). In DDR1a and DDR1b, the gatekeeper residues are T664 and T701, respectively. When the gatekeeper residues are mutated to Ala or Gly, the mutant kinases have larger ATP-binding pockets than wild-type DDR1. As a result, the mutant enzymes ought to be more sensitive to protein kinase inhibitors such as 1NM-PP1 (103). This approach allows the use of inhibitors such as 1NM-PP1 to mimic the effects of a specific DDR1 inhibitor. We mutated the gatekeeper residues in DDR1a and DDR1b to either Gly or Ala and expressed the mutants fused to mEGFP in PSN1 cells, a human pancreatic cancer cell line lacking endogenous DDR1 (Figure 7). The mutants with Gly in the gatekeeper position were no longer active (results not shown) while those with Ala in the gatekeeper position were activated by collagen.

Collagen I-induced tyrosine phosphorylation of DDR1a-mEGFP (T664A) and DDR1b-mEGFP (T701A) was inhibited by 1NM-PP1. Importantly, the collagen-dependent phosphorylation of wild-type DDR1a and DDR1b was not affected by the drug (Figure 7). We then performed Boyden chamber assays with Matrigel-coated filters to test the effects of the DDR1 isoforms with gatekeeper mutations on invasion of L3.6pl cells with endogenous DDR1 knocked down (Figure 8). We found DDR1b but not DDR1a promoted cell invasion, and this invasion was inhibited by 1NM-PP1. We plated the L3.6pl cells expressing the gatekeeper mutants on collagen I and found that in the presence of 1NM-PP1 DDR1b-mEGFP (T701A) failed to rescue the up-regulation of N-cadherin (Figure 9). The data show the kinase activity of DDR1b but not DDR1a is necessary to mediate collagen I-induced up-regulation of N-cadherin and to increase cell invasiveness.

Recently, specific inhibitors of DDR1 have been developed (104, 105). The specific inhibitor 7rh (86) inhibited collagen I-dependent up-regulation of N-cadherin (Figure 10), consistent with the results we obtained with 1NM-PP1 and the gatekeeper mutant form of DDR1b (Figure 9). As mentioned above, in pancreatic cancer cell lines we have shown collagen can signal through both integrins and DDR1 (41). L3.6pl cells respond to collagen almost exclusively through the DDR1

arm of this signaling pathway while the inhibition seen with 7rh in T3M-4 was partial, presumably due to signaling through integrins (Figure 10).

Figure 7. Collagen I-induced activation of the gatekeeper mutants of DDR1a and DDR1b is inhibited by 1NM-PP1.

(left panel) In contrast to T3M-4 cells, PSN1 cells do not express DDR1 so we used it for testing the sensitivity of the gatekeeper mutants to 1NM-PP1. (right panel) Wild-type DDR1a-mEGFP (lanes 1-4), wild-type DDR1b-mEGFP (lanes 9-12) or the gatekeeper mutants DDR1a-mEGFP T664A (lanes 5-8) and DDR1b-mEGFP T701A (lanes 13-16) were stably expressed in PSN1 cells. The cells were plated on tissue culture plastic (w/o col I) or collagen-coated plates (col I) for 18 hours and treated with DMSO (lanes 1, 2, 5, 6, 9, 10, 13, 14), 0.1 μM 1NM-PP1 (lanes 3, 7, 11, 15) or 1.0 μM 1NM-PP1 (lanes 4, 8, 12, 16). DDR1 was immunoprecipitated and the activity of DDR1 was measured by blotting with anti-phosphotyrosine.

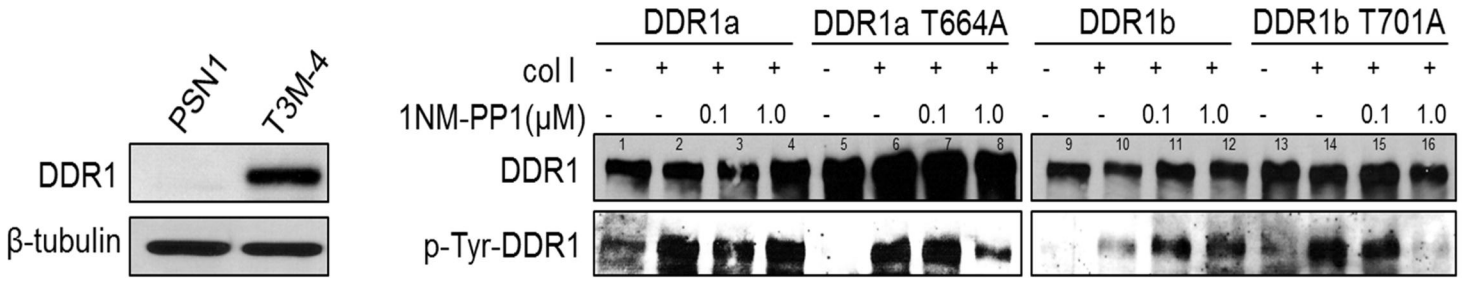
PSN1
T3M-4
DDR1
β-tubulin
DDR1a
DDR1a T664A
DDR1b
DDR1b T701A
col I
1NM-PP1(μM)
DDR1
p-Tyr-DDR1

Figure 8. Inhibiting DDR1b reduces pancreatic cancer cell invasiveness.

Boyden chamber assays were performed with L3.6pl cells expressing shRNA to EGFP or shRNA targeting DDR1 or knockdown cells expressing DDR1 gatekeeper mutants. 1.0 μM 1NM-PP1 inhibited the increased invasion seen in the knockdown cells expressing DDR1b T701A. The p values (n=3) in the graph reflect pairwise comparisons using Student's t-test. NS: not significant.

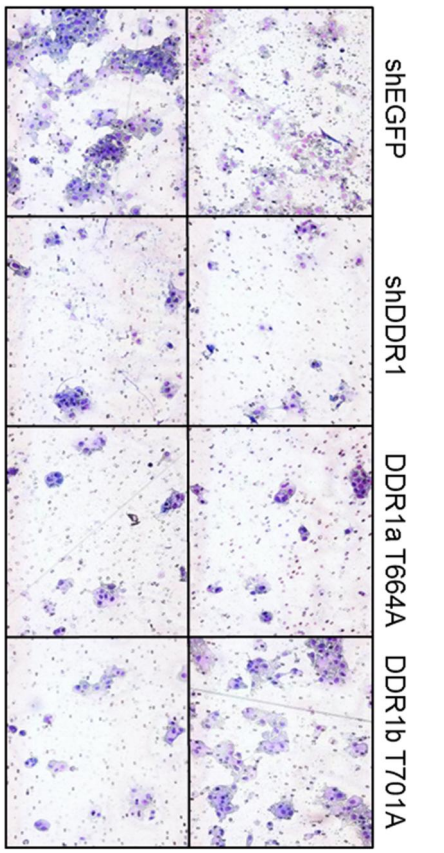
shEGFP
shDDR1
DDR1a T664A
DDR1b T701A
DMSO
1NM-PP1

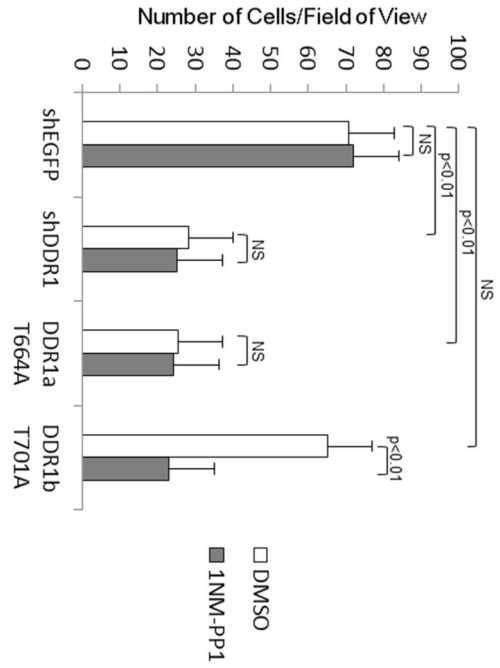
Number of Cells/Field of View
0
10
20
30
40
50
60
70
80
90
100
NS
p<0.01
NS
p<0.01
NS
NS
p<0.01
shEGFP
shDDR1
DDR1a T664A
DDR1b T701A
DMSO
1NM-PP1

Figure 9. Inhibiting DDR1b reduces collagen I-dependent up-regulation of N-cadherin.

L3.6pl cells were stably infected with constructs expressing shRNA to EGFP (lanes 1&9) or shRNA targeting DDR1 (lanes 2-8, 10-16). The gatekeeper mutants DDR1a-mEGFP T664A (lanes 3&7) or DDR1b-mEGFP (lanes 4&8) were stably expressed in the knockdown cells. Cells were plated on uncoated (lanes 1-8) or collagen-coated plates (lanes 9-16) for 18 hours and treated with DMSO (lanes 1, 2, 3, 6, 9, 10, 11, 14), 1.0 μM 1NM-PP1 (lanes 4, 7, 12, 15) or 10 μM 1NM-PP1 (lanes 5, 8, 13, 16). Cell extracts were blotted with antibodies for DDR1, E-cadherin, N-cadherin or β-tubulin. Asterisks indicate non-specific bands recognized by the DDR1 antiserum.

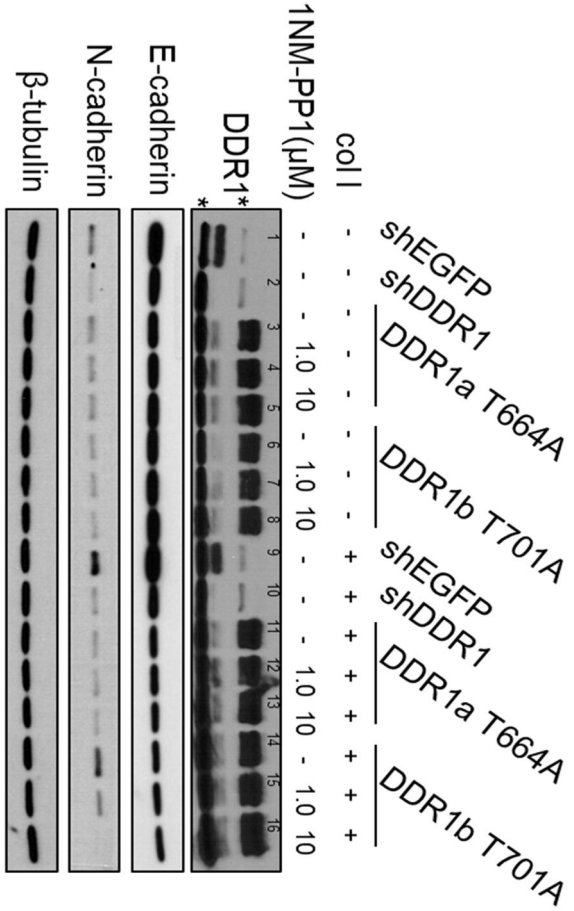
shEGFP
shDDR1
DDR1a T664A
DDR1b T701A
shEGFP
shDDR1
DDR1a T664A
DDR1b T701A
col I
1NM-PP1(μM)
DDR1*
*
E-cadherin
N-cadherin
β-tubulin

Figure 10. Collagen I-dependent up-regulation of N-cadherin can be inhibited by the specific DDR1 inhibitor.

L3.6pl or T3M-4 cells were plated on uncoated or collagen-coated plates for 18 hours and treated with DMSO or the specific DDR1 inhibitor 7rh. Cell extracts were blotted for N-cadherin or β-tubulin. In our previous studies, signaling though both DDR1 and beta1-integrin contributed to the collagen-dependent up-regulation of N-cadherin. The response of L3.6pl to collagen is strongly dependent upon signaling through the DDR1 arm of the pathway.

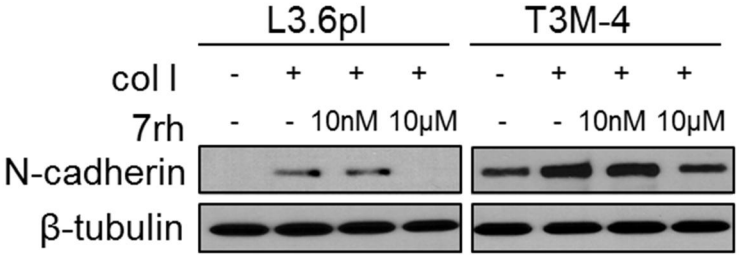
L3.6pl
T3M-4
col I
7rh
- + + + - + + +
- - 10nM 10μM - - 10nM 10μM
N-cadherin
β-tubulin

Chapter IV

Tyrosine513 of DDR1b Plays a Crucial Role in Collagen I-induced Up-regulation of N-cadherin

As we mentioned earlier, due to alternative splicing, DDR1b has an extra 37-residue segment in the cytosolic juxtamembrane region, which includes two tyrosines (Y513 and Y520) that are lacking in DDR1a. Since DDR1 is a tyrosine kinase, we focused on these tyrosines and constructed the DDR1b-mEGFP Y513F, Y520F and Y513F/Y520F (YFYF) mutants. The mutants as well as wild-type DDR1b-mEGFP were expressed in L3.6pl cells with endogenous DDR1 knocked down (Figure 11a). We found that up-regulation of N-cadherin was fully restored only when Y513 was intact.

Previously we showed that activation of JNK1 is necessary for collagen I-dependent up-regulation of N-cadherin (41) (Figure 2). Activation of JNK1 is indicated by the phosphorylation of T183 and Y185 (106). In knockdown cells, we found JNK1 was activated in response to collagen I when the knockdown cells expressed DDR1b-mEGFP but not when they expressed DDR1b-mEGFP Y513F (Figure 11b). This shows that Y513 of DDR1b is critical for collagen I-induced signaling to JNK1 and the resulting up-regulation of N-cadherin.

Figure 11. Tyr513 of DDR1b is required for collagen I-induced up-regulation of N-cadherin and activation of JNK1.

(a) Derivatives of L3.6pl cells were cultured on uncoated (w/o col I) or collagen-coated (col I) plates for 18 hours. Lysates were run on SDS gels and then blotted for DDR1, E-cadherin, N-cadherin or β-tubulin. Cells were infected with viral constructs expressing an shRNA targeting EGFP (lanes 1&7) or one targeting DDR1 (lanes 2-6, 8-12). Cells with DDR1 stably knocked down were then infected with viral constructs encoding wild-type or mutant DDR1b (lanes 3-6, 9-12) fused to mEGFP. Asterisks indicate non-specific bands recognized by the DDR1 antiserum. (b) The collagen I-induced activation of JNK1 was examined in the L3.6pl cell lines. Cells expressing an shRNA targeting DDR1 (lanes 2-7, 9-14) were infected with constructs encoding wild-type or mutant forms of DDR1b fused to mEGFP (lanes 3-7, 10-14) and cultured on uncoated (w/o col I) or collagen-coated plates (col I) for 18 hours. Lysates were run on SDS gels, and then blotted for JNK1 and phospho-JNK (Thr183/Tyr185). As a positive control for phospho-JNK, L3.6pl cells expressing an shRNA targeting EGFP were treated with anisomycin (25 μg/ml for 30 minutes) activating all the isoforms of JNK, which are recognized by the phospho-JNK antibodies.

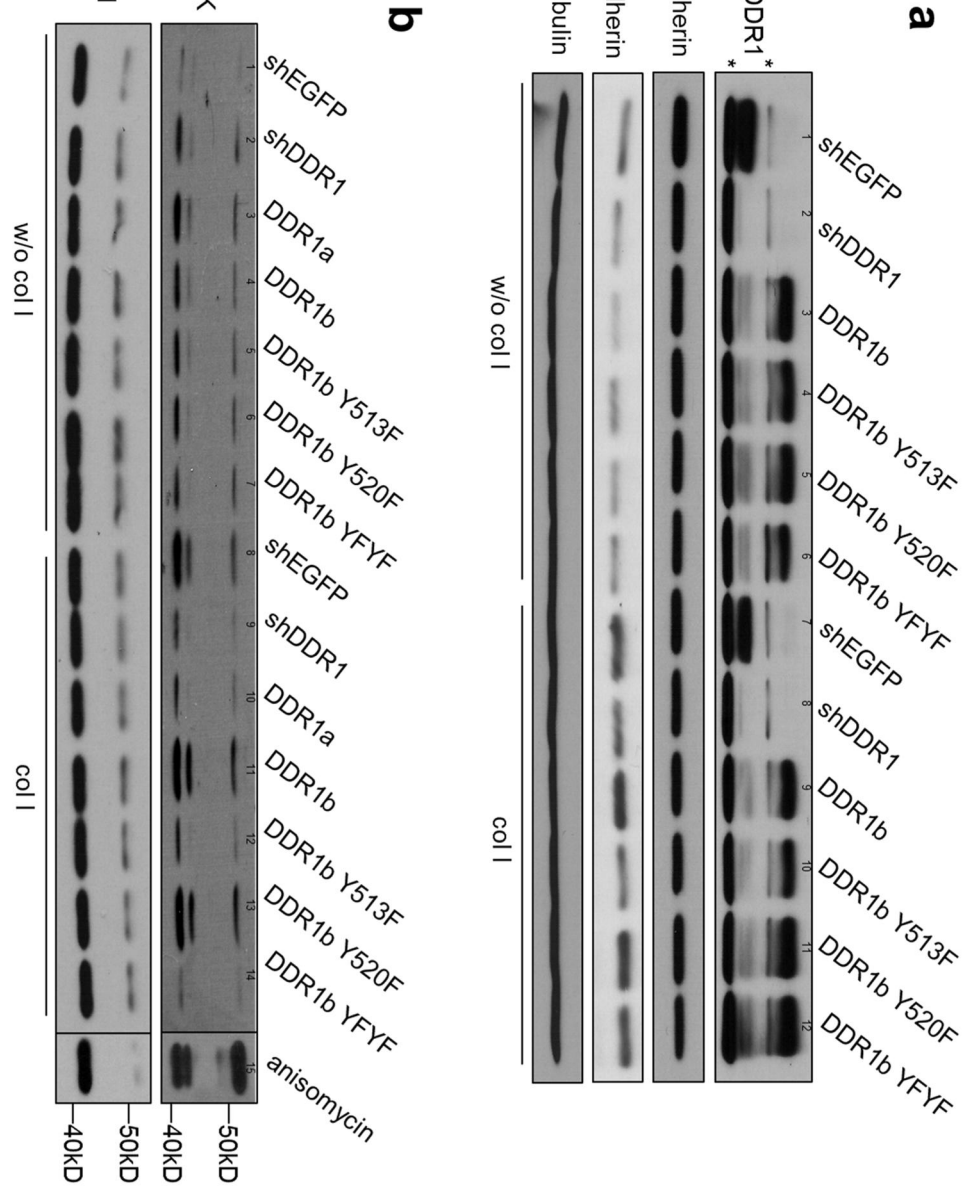
a
DDR1
E-cadherin
N-cadherin
β-tubulin
shEGFP
shDDR1
DDR1b
DDR1b Y513F
DDR1b Y520F
DDR1b YFYF
w/o col I
col I
b
p-JNK
JNK1
shEGFP
shDDR1
DDR1a
DDR1b
DDR1b Y513F
DDR1b Y520F
DDR1b YFYF
anisomycin
w/o col I
col I
50kD
40kD
50kD
40kD

Chapter V

Shc1 Interacts with Y513 of DDR1b through Its Phosphotyrosine Binding (PTB) Domain and the Interaction is Necessary for the Up-regulation of N-cadherin

Since Y513 is responsible for the collagen-I activated signaling pathway, we sought to determine which protein interacts with this residue to mediate the downstream signaling. Y513 of human DDR1 is in the sequence NPAY. Other mammalian species as well as the Xenopus (NP_001083540.1) and Zebrafish (XP_009290548.1) orthologues of DDR1 also have the sequence NPAY embedded in highly homologous sequences that are encoded by alternatively spliced exons (Figure 12).

Shc1 is a prototypical signaling adaptor with three isoforms (p66, p52 and p46) named according to relative molecular weight (107). All three isoforms of Shc1 have a C-terminal Src Homology (SH) 2 domain, which can bind to phosphotyrosine, as well as an N-terminal PTB domain, which also binds phosphotyrosine residues including phospho-Y513 of DDR1b (79, 108, 109). The two domains are connected by a central collagen homology (CH) 1 region containing consensus tyrosine residues that can be phosphorylated and serve as recognition motifs for other signaling effectors (110). The three isoforms share the same PTB-CH1-SH2 region and are only different at their N-termini. p46Shc1 and p52Shc1 are generated from the same transcript due to translation initiation at different start codons, while p66Shc1 is from a transcript initiated from a different promoter (111).

In order to determine if Shc1 interacts with DDR1b in pancreatic cancer cells, we performed co-immunoprecipitation assays. Only DDR1b-mEGFP was co-immunoprecipitated by antibodies to Shc1, and the interaction was collagen-dependent. Mutating Y513 largely prevented the co-immunoprecipitation (Figure 13). This suggested there was a direct collagen-dependent interaction between Y513 of DDR1b and Shc1. In order to determine if Shc1 was involved in the collagen I-induced signaling pathway leading to the up-regulation of N-cadherin, we knocked down Shc1 in L3.6pl cells with 4 different lentiviral shRNA targeting the 3'UTR, which is common to all the transcripts (Figure 14a). We found that up-regulation of N-cadherin in response to collagen I was eliminated by knocking down Shc1 (Figure 14b). We introduced

Figure 12. The NPAY sequences within the cytosolic juxtamembrane regions of DDR1b are highly homologous.

The extra 37 amino acids of human DDR1b are aligned with those of other species (XENLA = Xenopus laevis; DANRE = Danio rerio (zebrafish)). The NPAY sequences are in red. The amino acid sequences were aligned with UniProt.

```
SP|Q08345|DDR1_HUMAN    ALLLSNPAYRLLLATYARPPRGPGPPTPAWAKPTNT-Q 541
SP|Q03146|DDR1_MOUSE    ALLLSNPAYRLLLATYARPPRGPGPPTPAWAKPTNT-Q 539
TR|E1BBP4|E1BBP4_BOVIN  ALLLSNPAYRLLLATYARPPRGPGPPTPAWAKPTNT-Q 544
TR|Q6P9I0|Q6P9I0_XENLA5 ALLLNNPAYELLLTTYSRPITEHGGLQ---AKPVN--- 573
TR|E7F3X9|E7F3X9_DANRE  ALLLNNPAYHLLLSDLTHGPNRLTNCHSQQEKPLNLSQ 583
```

Figure 13. Shc1 interacts with Y513 of DDR1b in pancreatic cancer cells.

L3.6pl cells were infected with viral shRNA constructs targeting EGFP (lanes 1&8) or DDR1 (lanes 2-7 and 9-14). The DDR1 knockdown cells were then infected with viral constructs encoding various forms of DDR1 fused to mEGFP (lanes 3-7, 10-14). Endogenous Shc1 was immunoprecipitated, and the immunoprecipitates were blotted with antibodies to DDR1 or Shc1. The amount of DDR1 in the lysates is shown in the bottom panel. In some experiments, lysates of cells expressing DDR1-mEGFP fusion proteins had a protein migrating at the position of endogenous DDR1. However, these proteins only show collagen-dependent association with Shc1 if the full-length fusion protein does, suggesting they are not endogenous DDR1. An antibody against GFP did not recognize these bands but detected bands at the size expected for mEGFP (data not shown). These data are consistent with cleavage of the mEGFP tag from the fusion proteins.

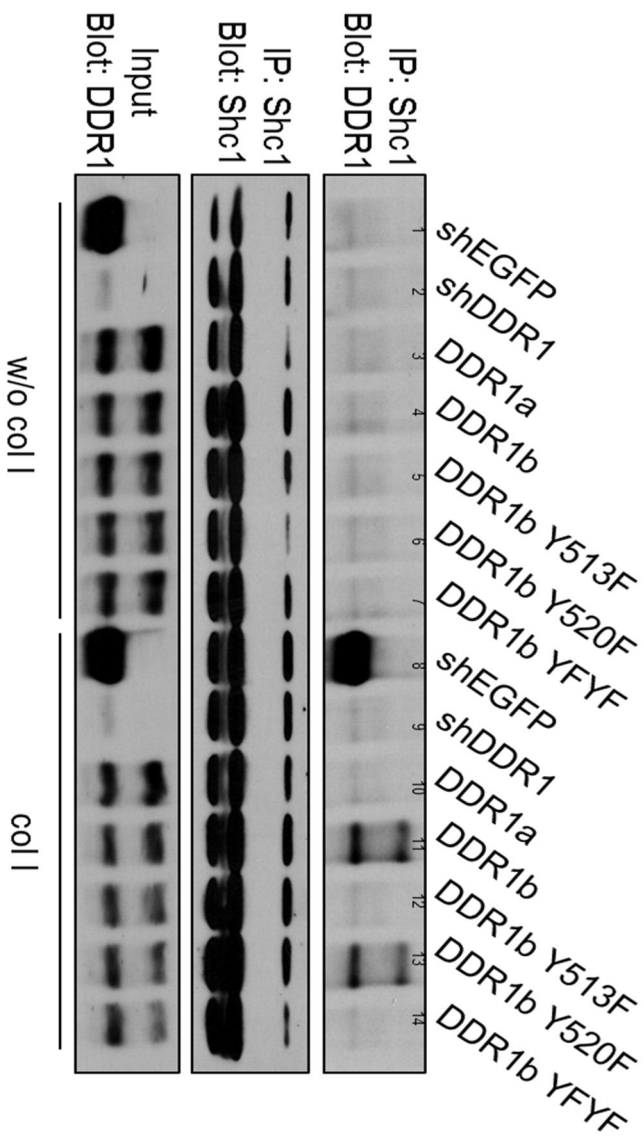
IP: Shc1
Blot: DDR1
IP: Shc1
Blot: Shc1
Input
Blot: DDR1
shEGFP
shDDR1
DDR1a
DDR1b
DDR1b Y513F
DDR1b Y520F
DDR1b YFYF
shEGFP
shDDR1
DDR1a
DDR1b
DDR1b Y513F
DDR1b Y520F
DDR1b YFYF
w/o col I
col I

Figure 14. DDR1b up-regulates N-cadherin through Shc1.

(a) Shc1 was knocked down in L3.6pl cells with 4 different shRNAs targeting the 3'UTR (shShc1 991, 997, 208, 434). shRNA targeting EGFP was used as a control. The three major protein isoforms of Shc1 (p66, p52 and p46, see Figure 16a) were detected. (b) Cells expressing shRNA targeting EGFP as well as Shc1 knockdown cells were cultured on uncoated (w/o col I) or collagen-coated plates (col I) for 18 hours. Lysates were run on SDS gels and blotted for N-cadherin or β-tubulin. Cells expressing shRNAs 208 and 434 were selected for further experiments.

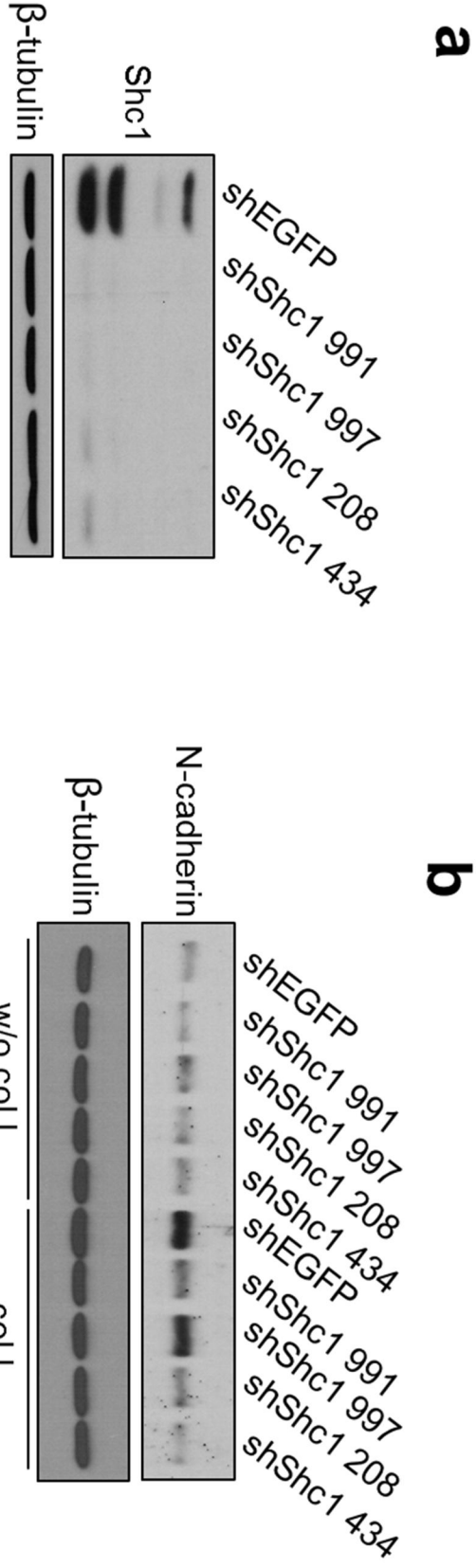
a
Shc1
β-tubulin
shEGFP
shShc1 991
shShc1 997
shShc1 208
shShc1 434
b
N-cadherin
β-tubulin
w/o col I
col I
shEGFP
shShc1 991
shShc1 997
shShc1 208
shShc1 434
shEGFP
shShc1 991
shShc1 997
shShc1 208
shShc1 434

p46Shc1, p52Shc1 or p66Shc1 into Shc1 knockdown cells and found that all three isoforms could rescue the up-regulation of N-cadherin induced by collagen I (Figure 15).

Point mutations have been identified that inactivate the PTB and SH2 domains of Shc1 (107). Using the amino acid numbers from mouse p52Shc1 (AAC52146.1), R175Q inactivates the PTB domain and R397K inactivates the SH2 domain (112). Phosphorylation of Y239/Y240 and Y313 of Shc1 is important in binding the SH2 domain of another adaptor protein Grb2 (113). We reintroduced 3X FLAG-tagged wild-type or mutated mouse p52Shc1 (R175Q, R397K, Y313F (mutant 1F), Y239F/Y240F (mutant 2F), Y239F/Y240F/Y313F (mutant 3F)) into L3.6pl cells with endogenous Shc1 knocked down, and found that only the PTB domain of Shc1 is necessary for collagen I-dependent up-regulation of N-cadherin. Neither inactivation of the SH2 domain nor mutation of the tyrosine residues prevented up-regulation of N-cadherin (Figure 16b). Since Y513 of DDR1b is within the Shc1 PTB domain consensus binding motif LLSNPAY (114), these results further support that up-regulation of N-cadherin induced by collagen I is mediated by interaction between Y513 of DDR1b and the PTB domain of Shc1.

Figure 15. All three isoforms of Shc1 rescued collagen I-dependent up-regulation of N-cadherin.

Cells expressing shRNA constructs targeting Shc1 (lanes 2-9, lanes 11-18) were stably infected with viral constructs encoding one of the isoforms of Shc1: p46Shc1 (lanes 4, 7, 13, 16), p52Shc1 (lanes 5, 8, 14, 17), or p66Shc1 (lanes 6, 9, 15, 18). Cells were cultured on uncoated (w/o col I) or collagen-coated plates (col I) for 18 hours. Cell extracts were blotted with antibodies for N-cadherin or β-tubulin.

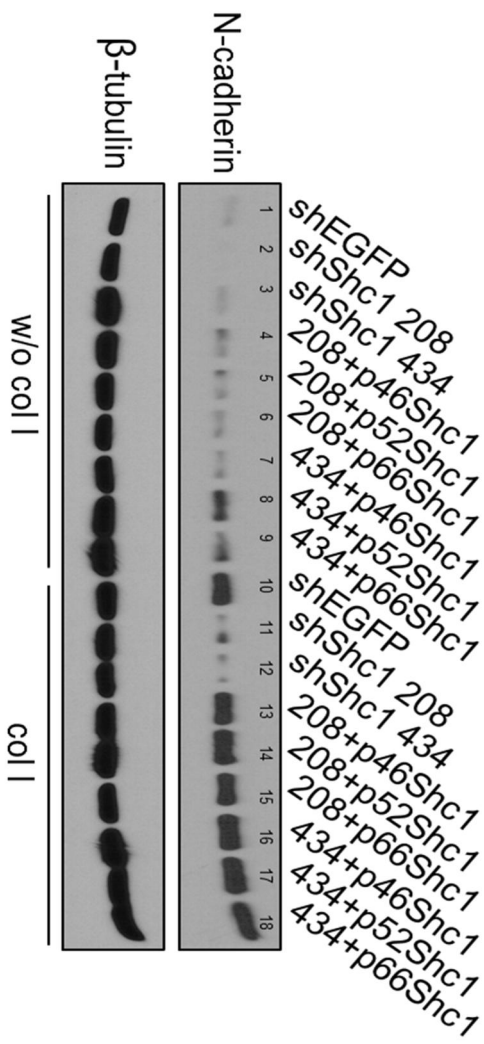
shEGFP
shShc1 208
shShc1 434
208+p46Shc1
208+p52Shc1
208+p66Shc1
434+p46Shc1
434+p52Shc1
434+p66Shc1
shEGFP
shShc1 208
shShc1 434
208+p46Shc1
208+p52Shc1
208+p66Shc1
434+p46Shc1
434+p52Shc1
434+p66Shc1
1 2 3 4 5 6 7 8 9 10 11 12 13 14 15 16 17 18
N-cadherin
β-tubulin
w/o col I
col I

Figure 16. A functional PTB domain of Shc1 is necessary for collagen I-induced up-regulation of N-cadherin.

(a) Schematic representation of p66Shc1, p52Shc1 and p46Shc1. In mouse p52Shc1 (AAC52146.1) R175Q inactivates the PTB domain and R397K inactivates the SH2 domain. Y239/Y240 and Y313 are consensus sites for phosphorylation-dependent binding to scaffold proteins such as Grb2. (b) L3.6pl cells were infected with shRNAs targeting either EGFP (lanes 1&9) or Shc1 (shShc1 208, lanes 2-8, 10-16). The Shc1 knockdown cells were then infected with various constructs of mouse p52Shc1. Constructs labeled with "YF" have one or more Y residues mutated to F. YF indicates Y313F; 2YF indicates Y239F/Y240F; and 3YF means mutation of all three residues. The cells stably expressing these constructs were then cultured on uncoated (w/o col I) or collagen-coated plates (col I). Cell extracts were blotted with antibodies for N-cadherin or β-tubulin. Only inactivation of the PTB domain prevented collagen-dependent up-regulation of N-cadherin.

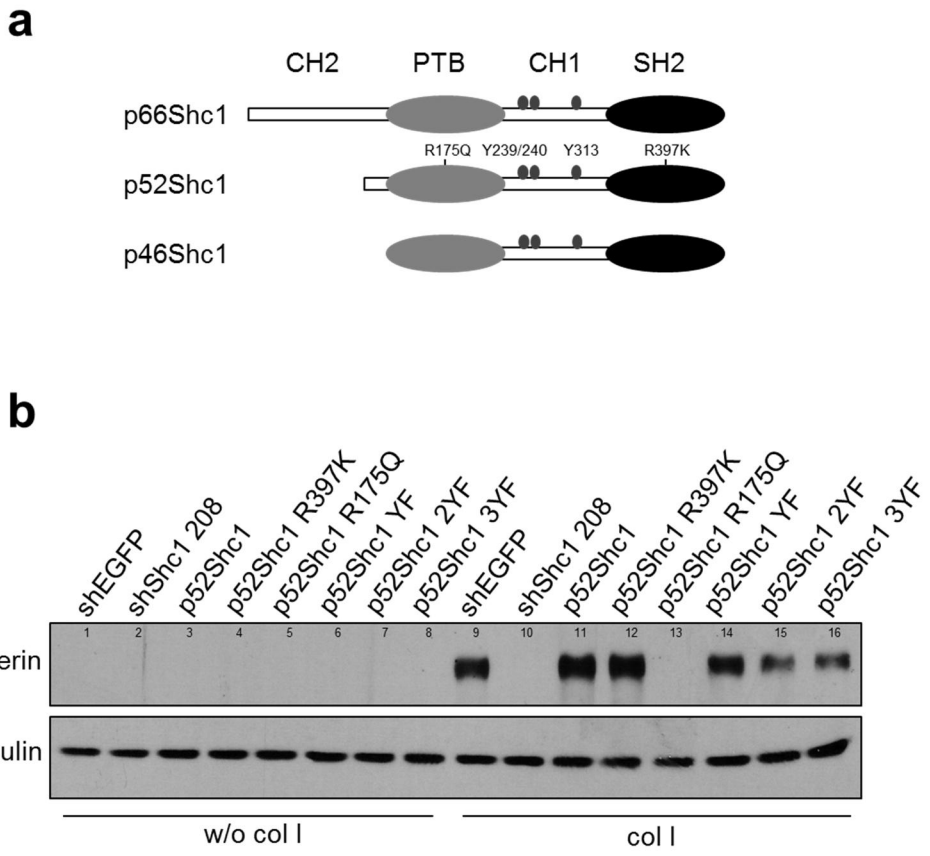
a
CH2
PTB
CH1
SH2
p66Shc1
R175Q
Y239/240
Y313
R397K
p52Shc1
p46Shc1
b
shEGFP
shShc1 208
p52Shc1
p52Shc1 R397K
p52Shc1 R175Q
p52Shc1 YF
p52Shc1 2YF
p52Shc1 3YF
1
2
3
4
5
6
7
8
9
10
11
12
13
14
15
16
N-cadherin
β-tubulin
w/o col I
col I

Chapter VI

In the Collagen I-induced Up-regulation of N-cadherin Shc1 Interacts with Pyk2

In the collagen I-induced up-regulation of N-cadherin signaling pathway, we have shown that Proline-rich tyrosine kinase 2 (Pyk2) is downstream of DDR1 (41). The structure of Pyk2 includes an N-terminal protein 4.1, ezrin, radixin, moesin (FERM) domain, a central kinase domain, two proline rich motifs (PR1, PR2), and a C-terminal focal adhesion targeting (FAT) domain (Figure 21a) (115, 116). Using endogenous proteins in L3.6pl cells, we observed collagen I-dependent association between DDR1 and Pyk2 (Figure 17a, lanes 1 and 8). Using L3.6pl cells with endogenous DDR1 knocked down, we showed that Y513 of DDR1b is necessary for the collagen I-dependent co-immunoprecipitation of DDR1b and Pyk2 (Figure 17a).

In order to determine if Shc1 provides the connection between endogenous DDR1 and Pyk2, we performed co-immunoprecipitations with an antibody to Shc1 using lysates from L3.6pl cells. We found the interaction between endogenous Shc1 and Pyk2 was detectable even in the absence of collagen, but exposure to collagen dramatically enhanced the interaction (Figure 17c, lanes 1 and 8). In addition, Pyk2 that co-immunoprecipitated with Shc1 following exposure of cells to collagen I was activated, as shown by an increased signal with anti-phosphoY402 antibodies. We also observed that Y513 of DDR1b is necessary for the strong association between Shc1 and Pyk2 (Figure 17c).

When they were transiently expressed in Phoenix cells (a derivative of HEK293T (89)), Shc1 and Pyk2 co-immunoprecipitated with one another. We took advantage of this to more carefully characterize the interaction between Shc1 and Pyk2. We transiently expressed the three different isoforms of mouse Shc1 together with wild-type rat Pyk2 (NP_059014, 1009 aa, with a C-terminal myc tag) or the Pyk2 mutants Y402F and K457A (kinase dead, (117)) in Phoenix cells (Figure 17b). Phosphorylation at Y402 of Pyk2 provides a binding site for the SH2 domain of Src-family tyrosine kinases. The recruitment of Src-family kinases leads to phosphorylation of Y579 and Y580 within the activation loop, which increases Pyk2 kinase activity (118-120).

We found that all three Shc1 isoforms interact with Pyk2 (Figure 17b), which is consistent with our earlier finding that all three isoforms of Shc1 rescue collagen-dependent up-regulation of N-cadherin (Figure 15). The interaction of Shc1 with full-length Pyk2 was not dependent on Y402 but was dependent on the kinase activity of Pyk2 (Figure 17b). We also tested a rat Pyk2 construct with L176A/Q177A mutations in the FERM domain that disrupt the interaction of Pyk2 with calmodulin (121) and found Shc1 interacted with this mutant (not shown) suggesting that calcium signaling is not playing a major role in the collagen-dependent interaction between Shc1 and Pyk2.

We transiently expressed Pyk2 and 3X FLAG-tagged wild-type or mutated mouse p52Shc (R175Q, R397K, Y313F, Y239F/Y240F, Y239F/Y240F/Y313F) in Phoenix cells and performed co-immunoprecipitations (Figure 17d). We found that all the mutated forms of p52Shc1 interacted with Pyk2. Thus we ruled out the possibilities that Pyk2 interacts with the PTB or SH2 domains of Shc1. In addition, the interaction between Pyk2 and the 3F mutant of Shc1 strongly suggests the interaction between Shc1 and Pyk2 is not mediated by Grb2, since Grb2 is known to couple to one or more of these sites. We do not know why kinase-dead Pyk2 failed to bind Shc1, especially since further mapping (see below) showed the kinase domain itself was not needed for the interaction between Shc1 and Pyk2. We also observed a significant signal for phosphorylated Y402 when Phoenix cells expressed the kinase-dead mutant. Even though it is commonly thought to be an autophosphorylation site, these data suggest endogenous tyrosine kinases can phosphorylate Y402 in the kinase-dead construct. One candidate is endogenous Pyk2, although Phoenix cells express relatively low levels of endogenous Pyk2 (Figure 18). The signal with anti-phosphoY402 seen in cells expressing the Y402F mutant is probably due to endogenous Pyk2 expressed by Phoenix cells. Other likely candidates are the Src-family kinases (120).

Figure 17. DDR1b and Shc1 interact with Pyk2, and collagen-dependent signaling via DDR1b strengthens the interaction.

(a) L3.6pl cells were infected with viral constructs encoding shRNAs targeting either EGFP (lanes 1&8) or DDR1 (lanes 2-7, 9-14). The DDR1 knockdown cells were then stably infected with viruses encoding various DDR1 constructs (lanes 3-7, 10-14). Cells were cultured on uncoated (w/o col I) or collagen-coated plates (col I) for 18 hours. DDR1 was immunoprecipitated and the immunoprecipitates were blotted with antibodies to Pyk2 or DDR1. Pyk2 exhibits collagen-dependent association with DDR1 that requires Y513. (b) p46Shc1 (lanes 1-3), p52Shc1 (lanes 4-6) or p66Shc1 (7-9) as well as either wild-type Pyk2 (lanes 1, 4, 7), Pyk2 Y402F (lanes 2, 5, 8), or Pyk2 KA (kinase dead, lanes 3, 6, 9) were transiently expressed in Phoenix cells. Immunoprecipitations were performed with an antibody against Shc1, and the immunoprecipitates were blotted with antibodies to Pyk2 or Shc1. As shown in the bottom two panels, cell lysates were blotted for total Pyk2 and phospho-Pyk2 (Tyr402). (c) L3.6pl cells expressing the same constructs as (a) were cultured on uncoated (w/o col I) or collagen-coated plates (col I) for 18 hours. Shc1 was immunoprecipitated and the immunoprecipitates were blotted with antibodies to Pyk2 or phospho-Pyk2 (Tyr402). The amount of endogenous Pyk2 in the lysates is shown in the bottom panel. The collagen-dependent association of Shc1 with Pyk2 requires Y513 of DDR1b. (d) Wild-type Pyk2 (lanes 1-7) as well as various p52Shc1 constructs tagged with 3X FLAG (lanes 1-6) were transiently expressed in Phoenix cells. Immunoprecipitations were performed with antibody against FLAG, and the immunoprecipitates were blotted with antibodies to Pyk2 or Shc1. The amount of total Pyk2 in the lysates is shown in the bottom panel. None of the mutations altered the association of Shc1 with Pyk2.

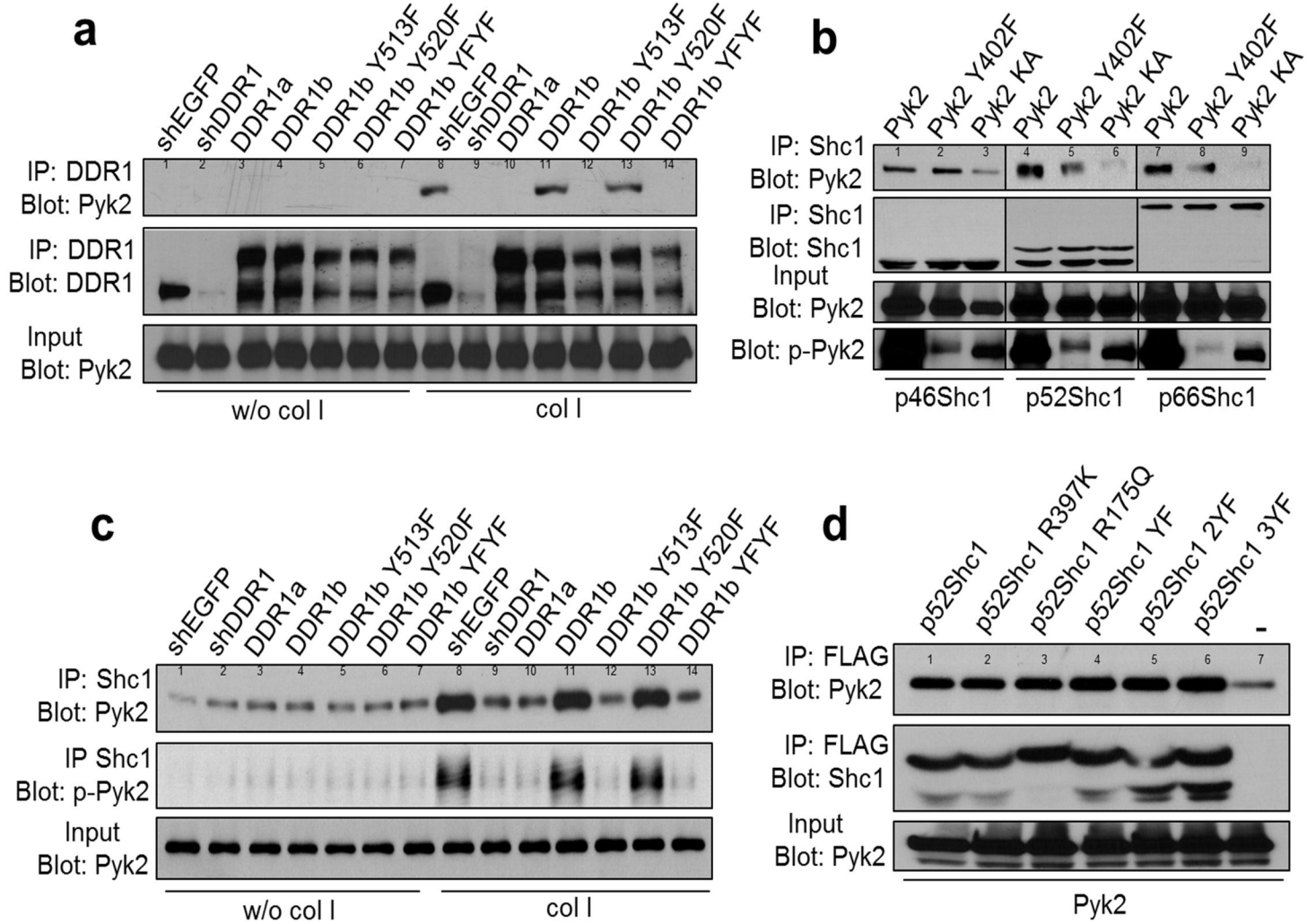
a
shEGFP
shDDR1
DDR1a
DDR1b
DDR1b Y513F
DDR1b Y520F
DDR1b YFYF
IP: DDR1
Blot: Pyk2
IP: DDR1
Blot: DDR1
Input
Blot: Pyk2
w/o col I
col I
b
Pyk2
Pyk2 Y402F
Pyk2 KA
IP: Shc1
Blot: Pyk2
IP: Shc1
Blot: Shc1
Input
Blot: Pyk2
Blot: p-Pyk2
p46Shc1
p52Shc1
p66Shc1
c
IP: Shc1
Blot: Pyk2
IP Shc1
Blot: p-Pyk2
Input
Blot: Pyk2
w/o col I
col I
d
p52Shc1
p52Shc1 R397K
p52Shc1 R175Q
p52Shc1 YF
p52Shc1 2YF
p52Shc1 3YF
-
IP: FLAG
Blot: Pyk2
IP: FLAG
Blot: Shc1
Input
Blot: Pyk2
Pyk2

Figure 18. Expression levels of Pyk2 and Shc1 in different cell lines.

(a) Cell extracts from parental L3.6pl, T3M-4, BxPC-3 and Phoenix cell lines were blotted with antibodies to Pyk2, Shc1 or β-tubulin as a loading control. (b) Pyk2 and p52Shc1 were transiently overexpressed in Phoenix cells. Cell extracts from these cells as well as parental Phoenix cells were blotted with antibodies for Pyk2, Shc1 and β-tubulin.

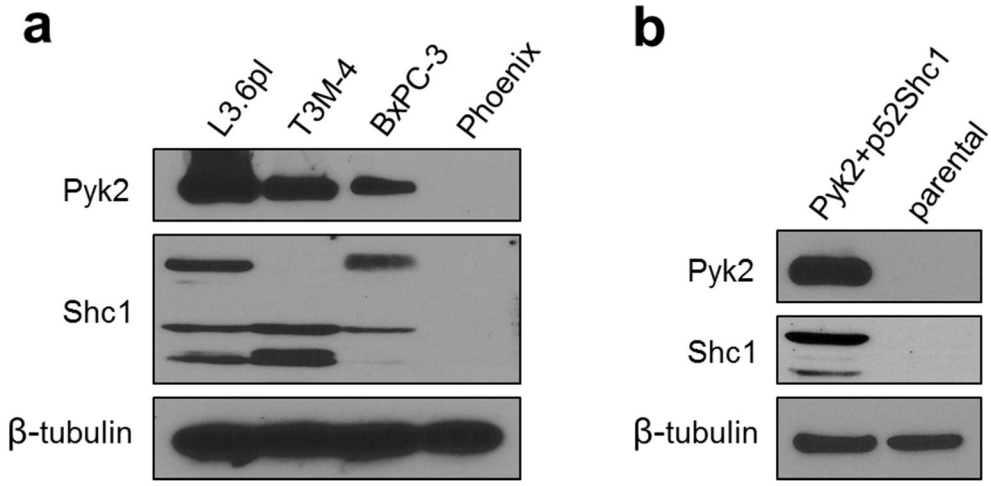
a
L3.6pl
T3M-4
BxPC-3
Phoenix
Pyk2
Shc1
β-tubulin
b
Pyk2+p52Shc1
parental
Pyk2
Shc1
β-tubulin

Chapter VII

A Short Sequence in the Central Domain of Shc1 is Necessary for the Interaction with the Proline-rich Region of Pyk2

Since neither the PTB nor SH2 domains of Shc1 are needed for its interaction with Pyk2, we made a series of truncated mouse p46Shc1 constructs (Figure 19a). We expressed Pyk2 and mouse 2X HA-tagged wild-type or truncated p46Shc1 (T1, T2, T3, T4, T5, T6, T7) in Phoenix cells and performed co-immunoprecipitations with an antibody against the HA tag (Figure 19b). We found that neither T1 nor T3 interacted with Pyk2 but T7, as well as the longer constructs, did. This indicates that interaction of mouse Shc1 with Pyk2 requires the sequence RPTLPSAQMS. Since the sequences of mouse and human Shc1 differ in this region (Figure 19a), we prepared truncated human Shc1 constructs and found the same region of human Shc1 was also required for the interaction between human Shc1 and Pyk2 (Figure 20).

We then transiently expressed different truncated Pyk2 constructs together with wild-type p46Shc1 in Phoenix cells to identify which region of Pyk2 interacts with Shc1 (Figure 21a). Co-immunoprecipitation was performed, and we found that amino acids 700-840 were necessary and sufficient for Pyk2 to interact with Shc1 (Figure 21b). This region contains 42 amino acids (aa 739-780) encoded by an alternatively spliced exon. The shorter Pyk2 isoform thus encodes 967 amino acids (122, 123). We inserted a mouse EST encoding amino acids 635-967 of the shorter isoform of Pyk2 into pEGFP-C2. Transient expression of this construct with p52Shc1 showed the two proteins still interacted (Figure 22). Thus Shc1 will interact with either isoform of Pyk2.

We tested if the interaction between Shc1 and Pyk2 is direct. We inserted a fragment encoding amino acids 700-840 of rat Pyk2 into pGST-Parallel and truncations T3 and T5 of mouse p46Shc1 into pMPB-Parallel (96) and purified the fusion proteins from E. coli. We incubated the two fusion proteins together but found no evidence for a direct interaction (Figure 23a). Using transient transfections, we then co-expressed Pyk2, p52Shc1 and either Grb2, CrkII or Nck1 in Phoenix cells to determine if one of these scaffolds could mediate the interaction between Shc1 and Pyk2. We found no evidence that one of these scaffolds serves to link Shc1 with Pyk2 (Figure 23b).

Overall, the interaction between Pyk2 and Shc1 requires a portion of the proline-rich region of Pyk2 and a small region in the central linker of Shc1 that has not previously been identified as interacting with a partner protein. The interaction between Shc1 and Pyk2 is not mediated by any of the common adaptors that function downstream of receptor tyrosine kinases.

Figure 19. A short segment of the central domain of Shc1 is necessary for the interaction with Pyk2.

(a) Shown are schematic representations of the p46Shc1 constructs (p46Shc1, T1-T7). Numbers on the right represent the last amino acid of the truncated protein using the amino acid numbers of mouse p52Shc1 (NP_035498.2). Portions of the sequences of mouse and human Shc1 are aligned and the boundaries of truncations T3, T6 and T7 are shown. The amino acids necessary for human and mouse Shc1 to interact with Pyk2 are underlined. (b) Wild-type Pyk2 (lanes 1-13) as well as various p46Shc1 constructs tagged with 2X HA (lanes 1-3, 5-8, 10-12) were transiently expressed in Phoenix cells. Immunoprecipitations were performed with antibody against HA, and the immunoprecipitates were blotted with antibodies to Pyk2 or HA. The amount of total Pyk2 in the lysates is shown in the bottom panel.

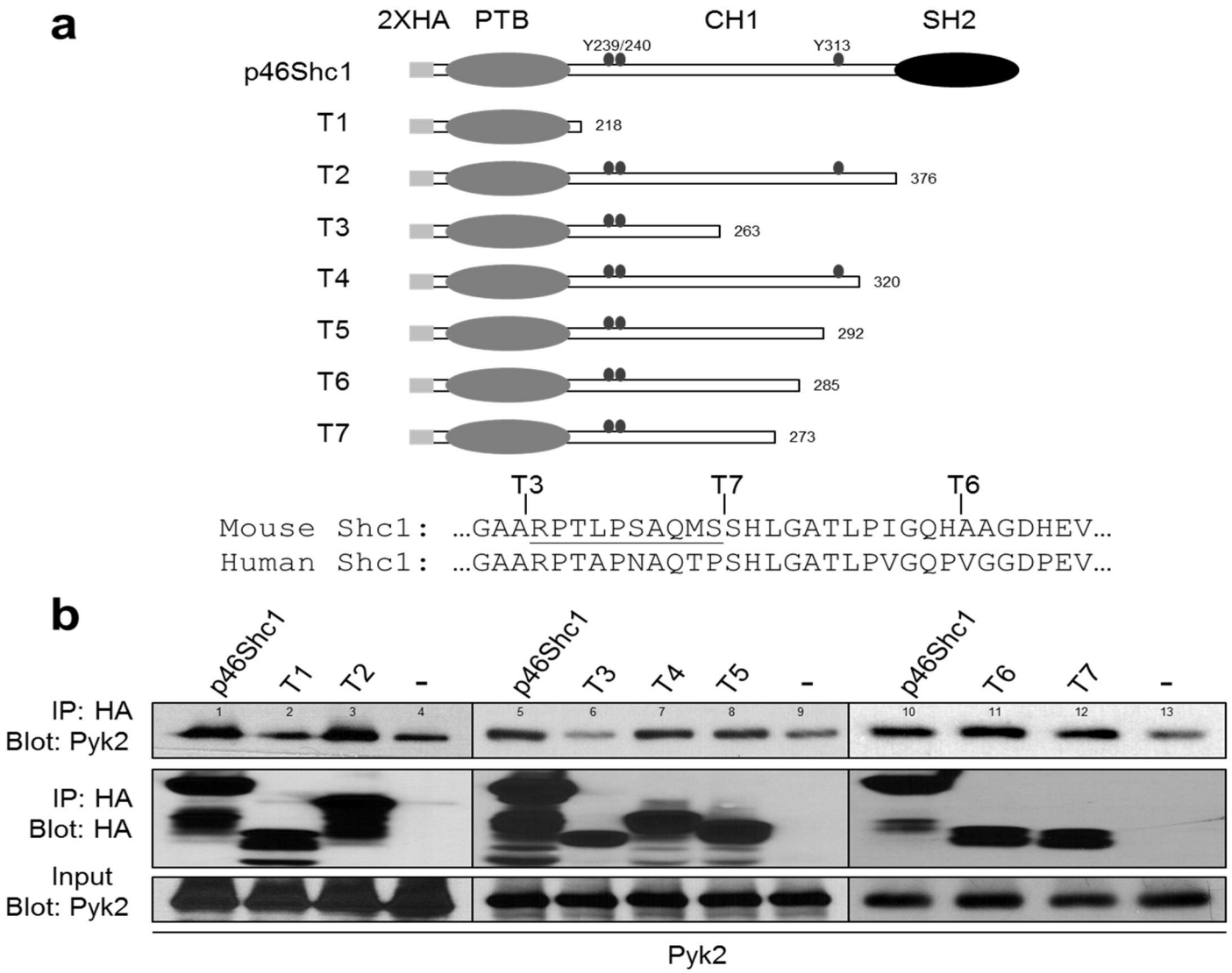
a
2XHA
PTB
CH1
SH2
Y239/240
Y313
p46Shc1
T1
218
T2
376
T3
263
T4
320
T5
292
T6
285
T7
273
T3
T7
T6
Mouse Shc1: ...GAARPTLPSAQMSSHLGATLPIGQHAAGDHEV...
Human Shc1: ...GAARPTAPNAQTPSHLGATLPVGQPVGGDPEV...
b
p46Shc1
T1
T2
-
p46Shc1
T3
T4
T5
-
p46Shc1
T6
T7
-
IP: HA
Blot: Pyk2
1
2
3
4
5
6
7
8
9
10
11
12
13
IP: HA
Blot: HA
Input
Blot: Pyk2
Pyk2

Figure 20. Human truncated p46Shc1 mutants T6 and T7 also interact with Pyk2.

Wild-type Pyk2 as well as mouse wild-type p46Shc1 (Msp46Shc1), human T6 or T7 p46Shc1 truncated mutant (HuT6 or HuT7) constructs tagged with 2X HA were transiently overexpressed in Phoenix cells. Immunoprecipitation was performed with antibody against HA, and the immunoprecipitates were blotted with antibodies to Pyk2 or HA. The amount of total Pyk2 in the lysates is shown in the bottom panel.

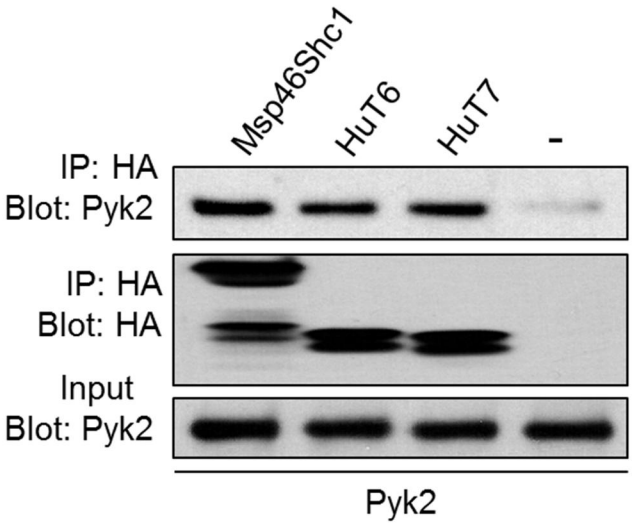
Msp46Shc1
HuT6
HuT7
-
IP: HA
Blot: Pyk2
IP: HA
Blot: HA
Input
Blot: Pyk2
Pyk2

Figure 21. The proline-rich region of Pyk2 interacts with Shc1.

(a) Schematic representations of wild-type rat Pyk2 and the various constructs are shown. The FERM, kinase and FAT domains are indicated. ASE represents the amino acids encoded by the alternatively spliced exon. PR1 and PR2 indicate proline-rich sequences. All the Pyk2 constructs were N-terminally tagged with GFP (thin box). (b) Wild-type p46Shc1 tagged with 2X HA (lanes 1-6) as well as various Pyk2 constructs (lanes 1-12) were transiently expressed in Phoenix cells. Immunoprecipitations were performed with an antibody against HA, and the immunoprecipitates were blotted with antibodies to GFP or HA. The amount of total Pyk2 variants in the lysates is shown in the bottom panel. Amino acids 700-840 of Pyk2 are necessary and sufficient for the interaction with Shc1.

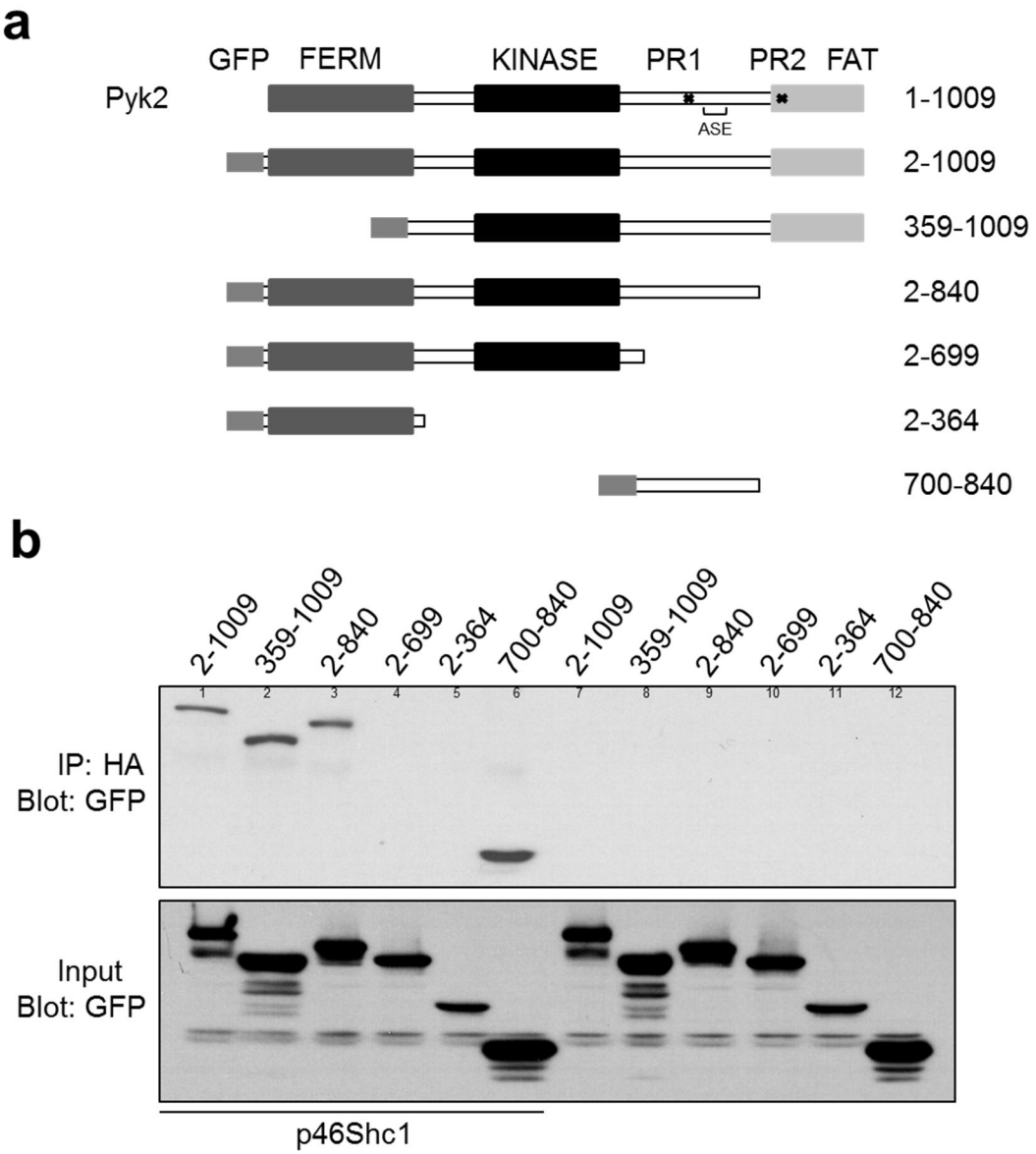
a
GFP
FERM
KINASE
PR1
PR2
FAT
Pyk2
ASE
1-1009
2-1009
359-1009
2-840
2-699
2-364
700-840
b
2-1009
359-1009
2-840
2-699
2-364
700-840
2-1009
359-1009
2-840
2-699
2-364
700-840
1
2
3
4
5
6
7
8
9
10
11
12
IP: HA
Blot: GFP
Input
Blot: GFP
p46Shc1

Figure 22. The shorter isoform of Pyk2 interacts with Shc1.

Pyk2 (full-length rat Pyk2) or Pyk2 short (mouse EST encoding amino acids 635-967 of the shorter isoform of Pyk2) was transiently expressed in Phoenix cells with or without wild-type p52Shc1 tagged with 3X FLAG. Immunoprecipitations were performed with an antibody against FLAG, and the immunoprecipitates were blotted with antibodies to Pyk2. The amount of total Pyk2 isoforms in the lysates is shown in the bottom panel.

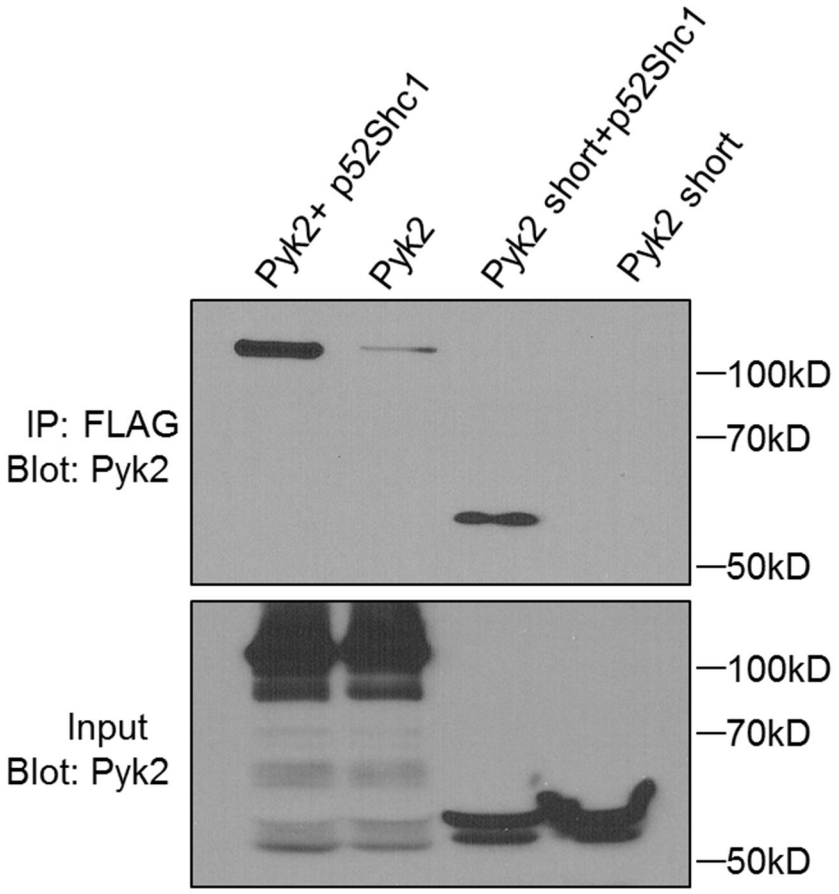
Pyk2+ p52Shc1
Pyk2
Pyk2 short+p52Shc1
Pyk2 short
IP: FLAG
Blot: Pyk2
—100kD
—70kD
—50kD
Input
Blot: Pyk2
—100kD
—70kD
—50kD

Figure 23. The interaction between Shc1 and Pyk2 is not direct.

(a) GST-Pyk2' (amino acids 700-840 of rat Pyk2 N-terminally tagged with GST) and truncations T3 and T5 of mouse p46Shc1 (see Figure 19a) N-terminally fused with Maltose Binding Protein (MBP) were purified from lysates of E. coli (input). Purified GST-Pyk2' was incubated with glutathione Sepharose beads. The washed beads were then incubated with buffer alone or with purified MBP-T3 or MBP-T5, pelleted, washed and solubilized in SDS sample buffer. The SDS-PAGE gel was stained with Coomassie Blue. GST-Pyk2' did not interact with MBP-T5, suggesting the interaction between Shc1 and Pyk2 is not direct. (b) Several candidate scaffolds that could mediate the interaction between Shc1 and Pyk2 were tested, but none promoted the interaction. Full-length rat Pyk2, as well as 3X FLAG-tagged mouse p52Shc1 in combination with one of the scaffold proteins Grb2, CrkII, or Nck1 (all human), were transiently expressed in Phoenix cells. Immunoprecipitations were performed with an antibody against Shc1, and the immunoprecipitates were blotted with antibodies to Pyk2 or Shc1. The amount of total Pyk2 in the lysates is shown in the bottom panel. None of the scaffold proteins increased the association between Shc1 and Pyk2.

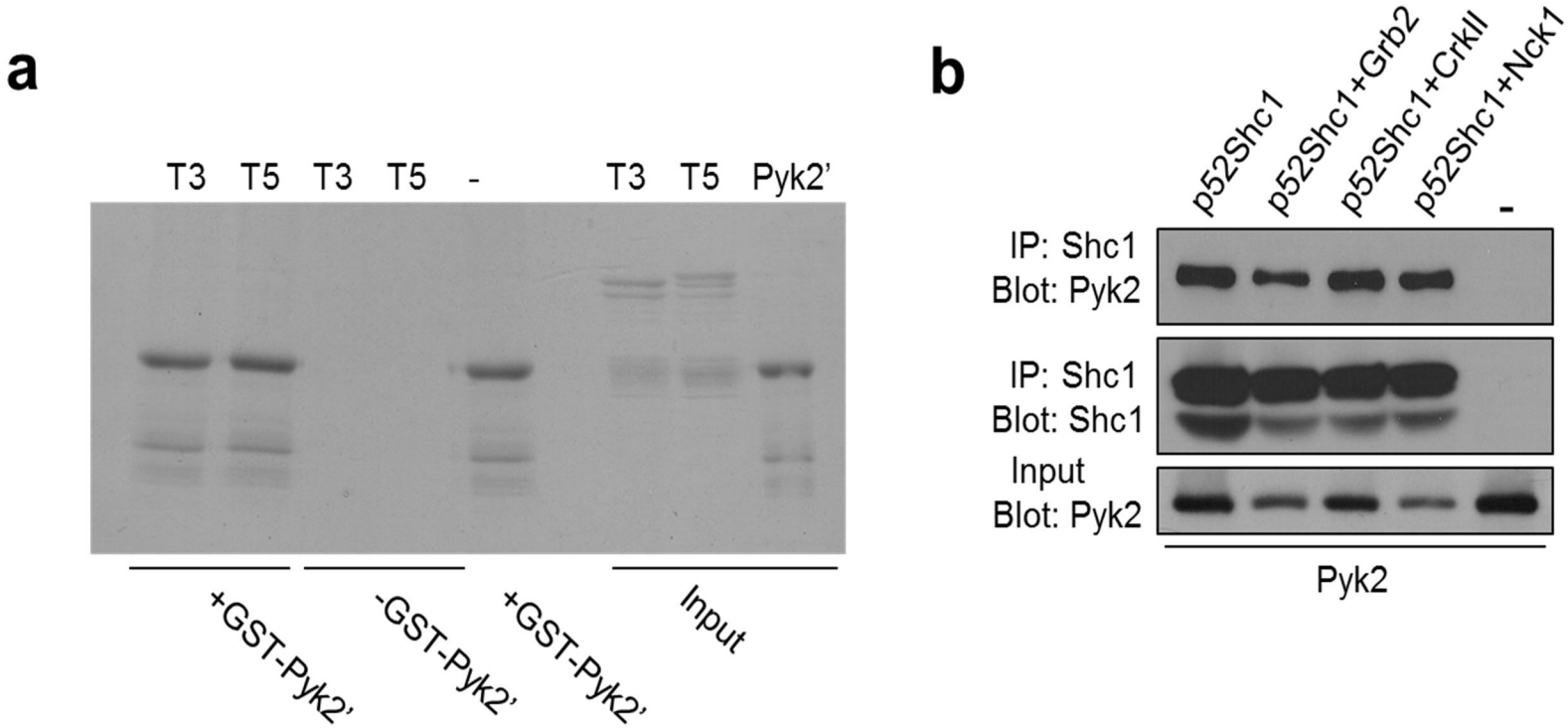
a
T3
T5
T3
T5
-
T3
T5
Pyk2'
+GST-Pyk2'
-GST-Pyk2'
+GST-Pyk2'
Input
b
p52Shc1
p52Shc1+Grb2
p52Shc1+CrkII
p52Shc1+Nck1
-
IP: Shc1
Blot: Pyk2
IP: Shc1
Blot: Shc1
Input
Blot: Pyk2
Pyk2

Chapter VIII

Discussion and Future Directions

Despite progress made in cancer biology and the development of new therapeutic strategies, the prognosis of patients with pancreatic cancer remains poor. Since EMT is important in the progression of pancreatic cancer, combining standard chemotherapy with inhibitors of EMT may hold some promise (39). Pancreatic cancer is characterized by extensive deposition of collagen I which can initiate EMT through activating DDR1 (81). Thus, targeting collagen I-induced EMT through inhibiting DDR1 may be a therapeutic option in pancreatic cancer.

To determine if the kinase activity of DDR1 was needed for collagen-dependent up-regulation of N-cadherin, we used the approach pioneered by the Shokat laboratory (103). We found when its gatekeeper residue was mutated to Ala, DDR1 retained collagen-dependent kinase activity and that 1NM-PP1 inhibited the collagen-dependent activation of mutant but not wild-type DDR1 (Figure 7). Specifically inhibiting the kinase activity of the gatekeeper-mutant form of DDR1b with 1NM-PP1 inhibited collagen-dependent cell migration as well as collagen-dependent up-regulation of N-cadherin (Figure 8&9). Recently, small molecule inhibitors specifically targeting the kinase activity of DDR1 have been developed (104, 105). Importantly, the DDR1-specific inhibitor 7rh (124) inhibited collagen-I induced N-cadherin up-regulation in pancreatic cancer cells (Figure 10). We have shown that signaling through both beta1-integrins and DDR1 contributes to collagen-dependent up-regulation of N-cadherin (41). Thus, inhibiting only the DDR1 arm of the pathway would typically be expected to only partially block the up-regulation of N-cadherin.

Knocking down DDR1 in lung cancer cells reduced cell survival, homing, and colonization in bone metastasis (125). In K-Ras-mutant lung cancers, Ambrogio et al. (2016) showed that combining 7rh to inhibit DDR1 with a Notch inhibitor was effective (126). In addition Ali-Rahmani et al. have shown inhibiting DDR1 with 7rh in combination with an immunotoxin caused shrinkage of tumor xenografts (127). Aguilera et al. (128) used the KIC mouse model of pancreatic cancer to argue for the importance of collagen-dependent signaling through DDR1 in

their studies of anti-VEGF therapy. In our studies, we showed a strong correlation exists between the expression of DDR1 and N-cadherin in primary and metastatic pancreatic cancer tissues (Figure 4). However, the roles played by signaling through DDR1 in the progression of pancreatic cancer are not well characterized. In future studies it will be important to determine how effective specific inhibitors of DDR1 (such as 7rh) are in treating mouse models of pancreatic cancer. Such studies have been initiated with the KIC model (129) and are planned for the KPC model (130).

In studies with pancreatic cancer-derived cell lines, we previously found that activating DDR1 initiates a pathway leading to the up-regulation of N-cadherin and that Pyk2 is a downstream effector (41). In the experiments described here, we extended this work and found that up-regulation of N-cadherin was due to activation of the specific isoform DDR1b (Figure 6). After DDR1b is activated by collagen, Shc1 via its PTB domain is recruited to Tyrosine 513 of DDR1b, leading to the up-regulation of N-cadherin (Figures 11, 13-16). Our data suggests Shc1 is associated with Pyk2 even before the activation of DDR1, perhaps because of signaling through other receptor tyrosine kinases. However, the activation of DDR1 significantly increases the association between Shc1, Pyk2 and DDR1, resulting in the activation of Pyk2 (Figure 17).

Neither the SH2 domain nor any of the well-characterized tyrosine phosphorylation sites of Shc1 are necessary for its interaction with Pyk2 or for the collagen-dependent up-regulation of N-cadherin (Figures 16b&17d). Although Pyk2 Y402F interacts with Shc1, the kinase-dead mutant (K457A) of Pyk2 does not (Figure 17b). This result is somewhat surprising since the region of Pyk2 that interacts with Shc1 is in between the kinase and FAT domains. This region of Pyk2 has two proline-rich sequences but does not itself contain a recognizable domain.

Faure et al. (95) mapped several activities, such as nuclear accumulation of Pyk2 to the same region we identified. However, they found serine phosphorylation in the alternatively-spliced

region played a role (95). Thus in their studies, the shorter isoform of Pyk2 lacked the activities while we found the shorter isoform of Pyk2 still interacts with Shc1.

Our data suggest inhibiting Pyk2 may prevent the DDR1-dependent up-regulation of N-cadherin. Pyk2 knockout mice are viable and fertile (131) while knocking out FAK results in embryonic lethality (132), suggesting the selective inhibition of Pyk2 may have therapeutic advantages. In this regard, it is notable that recently inhibitors with strong selectivity for Pyk2 over FAK have been identified (133).

Using fusion proteins purified from E. coli, we showed the interaction between Shc1 and Pyk2 is probably not direct (Figure 23a). The short stretch of amino acids we identified in mouse and human Shc1 has a PxxP sequence (Figure 19), suggesting that an adaptor with 2 or more SH3 domains (134) could bridge Shc1 with the proline-rich sequences in Pyk2. We tested several candidate adaptors (Grb2, CrkII or Nck1), but none enhanced the association of Shc1 with Pyk2 (Figure 23b). In this context, it is worth noting that the PxxP motif in human and mouse Shc1 is not conserved in some mammalian species, plus the context of the PxxP in mouse and human Shc1 does not conform well with known consensus SH3-binding sequences (135). The details of how Shc1 interacts with Pyk2 are the subject of ongoing studies. It is important to note the region we identified in Shc1 is not conserved in Shc2, Shc3 or Shc4 (Figure 24) suggesting other family members cannot substitute for Shc1.

In summary, this study is the first to report that the b isoform of DDR1 mediates collagen-dependent up-regulation of N-cadherin in pancreatic cancer and the adaptor protein Shc1 is necessary in this process. Using an orthotopic model, we have previously shown a cyclic peptide N-cadherin antagonist suppresses pancreatic cancer progression (70). Since it may be advantageous to inhibit the up-regulation of N-cadherin rather than inhibit N-cadherin itself, we

will pursue using the kinase inhibitor 7rh in an orthotopic model of pancreatic cancer to determine if inhibiting the kinase activity of DDR1 provides any therapeutic benefit.

Figure 24. Alignment of portions of the 4 human Shc sequences.

Shown are portions of the 4 human Shc proteins in the vicinity of the region we identified (see Figure 19. The 10 amino acids we identified in Shc1 are underlined and in bold. In this region, there is no similarity between the family members, suggesting that other family members cannot substitute for Shc1 in mediating collagen-dependent up-regulation of N-cadherin. The amino acid sequences were aligned with ClustalW.

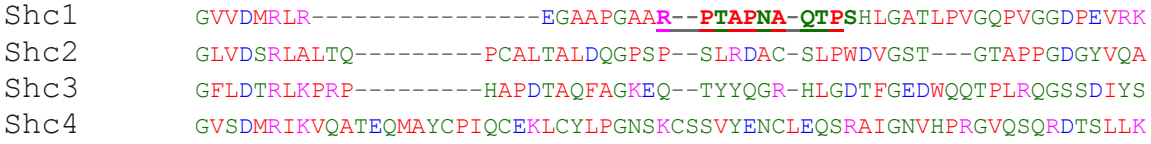
Shc1 GVVDMRLR----------EGAAPGAAR--PTAPNA-QTPSHLGATLPVGQPVGGDPEVRK
Shc2 GLVDSRLALTQ---------PCALTALDQGPSP--SLRDAC-SLPWDVGST---GTAPPGDGYVQA
Shc3 GFLDTRLKPRP---------HAPDTAQFAGKEQ--TYYQGR-HLGDTFGEDWQQTPLRQGSSDIYS
Shc4 GVSDMRIKVQATEQMAYCPIQCEKLCYLPGNSKCSSVYENCLEQSRAIGNVHPRGVQSQRDTSLLK

Chapter IX

Acknowledgements

The mouse anti-tubulin monoclonal antibody E7 developed by Drs. Michael McCutcheon and Sean Carroll was obtained from the Developmental Studies Hybridoma Bank, created by the NICHD of the NIH and maintained at The University of Iowa, Department of Biology, Iowa City, IA 52242. We thank Drs. Jean-Antoine Girault (Institut du Fer à Moulin, UMR-S839 Inserm and UPMC Paris), Teizo Yoshimura (National Cancer Institute, Bethesda, MD), Bruce Mayer (University of Connecticut Health Center, Farmington, CT), Wei Li (University of Southern California, Los Angeles, CA), Lee Graves (University of North Carolina at Chapel Hill, Chapel Hill, NC), Peter Siegel (McGill University, Montreal, Canada); Philip Tofilon (National Cancer Institute, Bethesda, MD); and Angie Rizzino, Rakesh Singh, Michel Ouellette and Tony Hollingsworth (University of Nebraska Medical Center, Omaha, NE) for reagents and cell lines. We thank Robin High (University of Nebraska Medical Center, Omaha, NE) for statistical analysis. These studies were supported by research grants from the National Institutes of Health (U54CA163120, S Batra PI; P50CA127297 and U01CA111294, MA Hollingsworth PI; P30CA036727, KH Cowan PI; R01GM051188, MJ Wheelock/KR Johnson PI; R21CA137401, KR Johnson PI and an Institutional Development Award (IDeA) from the National Institute of General Medical Sciences P30GM1063970 (to KR Johnson).

Chapter X

References

1. Gresham GK, Wells GA, Gill S, Cameron C, Jonker DJ. Chemotherapy regimens for advanced pancreatic cancer: a systematic review and network meta-analysis. BMC Cancer. 2014;14:471. Epub 2014/06/29.

2. Neoptolemos JP. Adjuvant treatment of pancreatic cancer. Eur J Cancer. 2011;47 Suppl 3:S378-80. Epub 2011/09/29.

3. Burris HA, 3rd, Moore MJ, Andersen J, Green MR, Rothenberg ML, Modiano MR, et al. Improvements in survival and clinical benefit with gemcitabine as first-line therapy for patients with advanced pancreas cancer: a randomized trial. J Clin Oncol. 1997;15(6):2403-13. Epub 1997/06/01.

4. Conroy T, Desseigne F, Ychou M, Bouche O, Guimbaud R, Becouarn Y, et al. FOLFIRINOX versus gemcitabine for metastatic pancreatic cancer. N Engl J Med. 2011;364(19):1817-25. Epub 2011/05/13.

5. Feig C, Gopinathan A, Neesse A, Chan DS, Cook N, Tuveson DA. The pancreas cancer microenvironment. Clin Cancer Res. 2012;18(16):4266-76. Epub 2012/08/17.

6. Neesse A, Michl P, Frese KK, Feig C, Cook N, Jacobetz MA, et al. Stromal biology and therapy in pancreatic cancer. Gut. 2011;60(6):861-8. Epub 2010/10/23.

7. Hwang RF, Moore T, Arumugam T, Ramachandran V, Amos KD, Rivera A, et al. Cancer-associated stromal fibroblasts promote pancreatic tumor progression. Cancer Res. 2008;68(3):918-26. Epub 2008/02/05.

8. Xu Z, Vonlaufen A, Phillips PA, Fiala-Beer E, Zhang X, Yang L, et al. Role of pancreatic stellate cells in pancreatic cancer metastasis. Am J Pathol. 2010;177(5):2585-96. Epub 2010/10/12.

9. Wehr AY, Furth EE, Sangar V, Blair IA, Yu KH. Analysis of the human pancreatic stellate cell secreted proteome. Pancreas. 2011;40(4):557-66. Epub 2011/04/19.

10. Phillips PA, McCarroll JA, Park S, Wu MJ, Pirola R, Korsten M, et al. Rat pancreatic stellate cells secrete matrix metalloproteinases: implications for extracellular matrix turnover. Gut. 2003;52(2):275-82. Epub 2003/01/14.

11. Rhim AD, Oberstein PE, Thomas DH, Mirek ET, Palermo CF, Sastra SA, et al. Stromal elements act to restrain, rather than support, pancreatic ductal adenocarcinoma. Cancer Cell. 2014;25(6):735-47. Epub 2014/05/27.

12. Ozdemir BC, Pentcheva-Hoang T, Carstens JL, Zheng X, Wu CC, Simpson TR, et al. Depletion of carcinoma-associated fibroblasts and fibrosis induces immunosuppression and accelerates pancreas cancer with reduced survival. Cancer Cell. 2014;25(6):719-34. Epub 2014/05/27.

13. Lee JJ, Perera RM, Wang H, Wu DC, Liu XS, Han S, et al. Stromal response to Hedgehog signaling restrains pancreatic cancer progression. Proc Natl Acad Sci U S A. 2014;111(30):E3091-100. Epub 2014/07/16.

14. Vonderheide RH, Bayne LJ. Inflammatory networks and immune surveillance of pancreatic carcinoma. Curr Opin Immunol. 2013;25(2):200-5. Epub 2013/02/21.

15. Pylayeva-Gupta Y, Lee KE, Hajdu CH, Miller G, Bar-Sagi D. Oncogenic Kras-induced GM-CSF production promotes the development of pancreatic neoplasia. Cancer Cell. 2012;21(6):836-47. Epub 2012/06/16.

16. Lesina M, Kurkowski MU, Ludes K, Rose-John S, Treiber M, Kloppel G, et al. Stat3/Socs3 activation by IL-6 transsignaling promotes progression of pancreatic intraepithelial neoplasia and development of pancreatic cancer. Cancer Cell. 2011;19(4):456-69. Epub 2011/04/13.

17. Provenzano PP, Cuevas C, Chang AE, Goel VK, Von Hoff DD, Hingorani SR. Enzymatic targeting of the stroma ablates physical barriers to treatment of pancreatic ductal adenocarcinoma. Cancer Cell. 2012;21(3):418-29. Epub 2012/03/24.

18. Ryan DP, Hong TS, Bardeesy N. Pancreatic adenocarcinoma. N Engl J Med. 2014;371(22):2140-1. Epub 2014/11/27.

19. Olive KP, Jacobetz MA, Davidson CJ, Gopinathan A, McIntyre D, Honess D, et al. Inhibition of Hedgehog signaling enhances delivery of chemotherapy in a mouse model of pancreatic cancer. Science. 2009;324(5933):1457-61. Epub 2009/05/23.

20. Merchant AA, Matsui W. Targeting Hedgehog--a cancer stem cell pathway. Clin Cancer Res. 2010;16(12):3130-40. Epub 2010/06/10.

21. Friess H, Yamanaka Y, Buchler M, Ebert M, Beger HG, Gold LI, et al. Enhanced expression of transforming growth factor beta isoforms in pancreatic cancer correlates with decreased survival. Gastroenterology. 1993;105(6):1846-56. Epub 1993/12/01.

22. Bachem MG, Schunemann M, Ramadani M, Siech M, Beger H, Buck A, et al. Pancreatic carcinoma cells induce fibrosis by stimulating proliferation and matrix synthesis of stellate cells. Gastroenterology. 2005;128(4):907-21. Epub 2005/04/13.

23. Hilbig A, Oettle H. Transforming growth factor beta in pancreatic cancer. Curr Pharm Biotechnol. 2011;12(12):2158-64. Epub 2011/05/31.

24. Hingorani SR, Harris WP, Beck JT, Berdov BA, Wagner SA, Pshevlotsky EM, et al. Phase Ib Study of PEGylated Recombinant Human Hyaluronidase and Gemcitabine in Patients with Advanced Pancreatic Cancer. Clin Cancer Res. 2016. Epub 2016/01/28.

25. Thiery JP, Acloque H, Huang RY, Nieto MA. Epithelial-mesenchymal transitions in development and disease. Cell. 2009;139(5):871-90. Epub 2009/12/01.

26. Acloque H, Adams MS, Fishwick K, Bronner-Fraser M, Nieto MA. Epithelial-mesenchymal transitions: the importance of changing cell state in development and disease. J Clin Invest. 2009;119(6):1438-49. Epub 2009/06/03.

27. Rhim AD, Mirek ET, Aiello NM, Maitra A, Bailey JM, McAllister F, et al. EMT and dissemination precede pancreatic tumor formation. Cell. 2012;148(1-2):349-61. Epub 2012/01/24.

28. Entenberg D, Kedrin D, Wyckoff J, Sahai E, Condeelis J, Segall JE. Imaging tumor cell movement in vivo. Curr Protoc Cell Biol. 2013;Chapter 19:Unit19 7. Epub 2013/03/05.

29. Raimondi C, Gradilone A, Naso G, Vincenzi B, Petracca A, Nicolazzo C, et al. Epithelial-mesenchymal transition and stemness features in circulating tumor cells from breast cancer patients. Breast Cancer Res Treat. 2011;130(2):449-55. Epub 2011/02/08.

30. Yu M, Bardia A, Wittner BS, Stott SL, Smas ME, Ting DT, et al. Circulating breast tumor cells exhibit dynamic changes in epithelial and mesenchymal composition. Science. 2013;339(6119):580-4. Epub 2013/02/02.

31. Brabletz T. EMT and MET in metastasis: where are the cancer stem cells? Cancer Cell. 2012;22(6):699-701. Epub 2012/12/15.

32. Kalluri R, Weinberg RA. The basics of epithelial-mesenchymal transition. J Clin Invest. 2009;119(6):1420-8. Epub 2009/06/03.

33. Giampieri S, Manning C, Hooper S, Jones L, Hill CS, Sahai E. Localized and reversible TGFbeta signalling switches breast cancer cells from cohesive to single cell motility. Nat Cell Biol. 2009;11(11):1287-96. Epub 2009/10/20.

34. Theveneau E, Marchant L, Kuriyama S, Gull M, Moepps B, Parsons M, et al. Collective chemotaxis requires contact-dependent cell polarity. Dev Cell. 2010;19(1):39-53. Epub 2010/07/21.

35. Sarrio D, Rodriguez-Pinilla SM, Hardisson D, Cano A, Moreno-Bueno G, Palacios J. Epithelial-mesenchymal transition in breast cancer relates to the basal-like phenotype. Cancer Res. 2008;68(4):989-97. Epub 2008/02/19.

36. Peinado H, Olmeda D, Cano A. Snail, Zeb and bHLH factors in tumour progression: an alliance against the epithelial phenotype? Nat Rev Cancer. 2007;7(6):415-28. Epub 2007/05/18.

37. Scheel C, Eaton EN, Li SH, Chaffer CL, Reinhardt F, Kah KJ, et al. Paracrine and autocrine signals induce and maintain mesenchymal and stem cell states in the breast. Cell. 2011;145(6):926-40. Epub 2011/06/15.

38. Marjanovic ND, Weinberg RA, Chaffer CL. Cell plasticity and heterogeneity in cancer. Clin Chem. 2013;59(1):168-79. Epub 2012/12/12.

39. Zheng X, Carstens JL, Kim J, Scheible M, Kaye J, Sugimoto H, et al. Epithelial-to-mesenchymal transition is dispensable for metastasis but induces chemoresistance in pancreatic cancer. Nature. 2015;527(7579):525-30. Epub 2015/11/13.

40. Vega S, Morales AV, Ocana OH, Valdes F, Fabregat I, Nieto MA. Snail blocks the cell cycle and confers resistance to cell death. Genes Dev. 2004;18(10):1131-43. Epub 2004/05/25.

41. Shintani Y, Fukumoto Y, Chaika N, Svoboda R, Wheelock MJ, Johnson KR. Collagen I-mediated up-regulation of N-cadherin requires cooperative signals from integrins and discoidin domain receptor 1. J Cell Biol. 2008;180(6):1277-89. Epub 2008/03/26.

42. Takeichi M. The cadherins: cell-cell adhesion molecules controlling animal morphogenesis. Development. 1988;102(4):639-55. Epub 1988/04/01.

43. Hirano S, Suzuki ST, Redies C. The cadherin superfamily in neural development: diversity, function and interaction with other molecules. Front Biosci. 2003;8:d306-55. Epub 2002/11/29.

44. Blaschuk OW, Sullivan R, David S, Pouliot Y. Identification of a cadherin cell adhesion recognition sequence. Dev Biol. 1990;139(1):227-9. Epub 1990/05/01.

45. Williams E, Williams G, Gour BJ, Blaschuk OW, Doherty P. A novel family of cyclic peptide antagonists suggests that N-cadherin specificity is determined by amino acids that flank the HAV motif. J Biol Chem. 2000;275(6):4007-12. Epub 2000/02/08.

46. Patel SD, Ciatto C, Chen CP, Bahna F, Rajebhosale M, Arkus N, et al. Type II cadherin ectodomain structures: implications for classical cadherin specificity. Cell. 2006;124(6):1255-68. Epub 2006/03/28.

47. Shan W, Yagita Y, Wang Z, Koch A, Fex Svenningsen A, Gruzglin E, et al. The minimal essential unit for cadherin-mediated intercellular adhesion comprises extracellular domains 1 and 2. J Biol Chem. 2004;279(53):55914-23. Epub 2004/10/16.

48. Kim JB, Islam S, Kim YJ, Prudoff RS, Sass KM, Wheelock MJ, et al. N-Cadherin extracellular repeat 4 mediates epithelial to mesenchymal transition and increased motility. J Cell Biol. 2000;151(6):1193-206. Epub 2000/12/21.

49. Suyama K, Shapiro I, Guttman M, Hazan RB. A signaling pathway leading to metastasis is controlled by N-cadherin and the FGF receptor. Cancer Cell. 2002;2(4):301-14. Epub 2002/10/26.

50. Su Y, Li J, Witkiewicz AK, Brennan D, Neill T, Talarico J, et al. N-cadherin haploinsufficiency increases survival in a mouse model of pancreatic cancer. Oncogene. 2012;31(41):4484-9. Epub 2011/12/14.

51. Orsulic S, Huber O, Aberle H, Arnold S, Kemler R. E-cadherin binding prevents beta-catenin nuclear localization and beta-catenin/LEF-1-mediated transactivation. J Cell Sci. 1999;112 (Pt 8):1237-45. Epub 1999/03/23.

52. Ohkubo T, Ozawa M. p120(ctn) binds to the membrane-proximal region of the E-cadherin cytoplasmic domain and is involved in modulation of adhesion activity. J Biol Chem. 1999;274(30):21409-15. Epub 1999/07/20.

53. Xiao K, Garner J, Buckley KM, Vincent PA, Chiasson CM, Dejana E, et al. p120-Catenin regulates clathrin-dependent endocytosis of VE-cadherin. Mol Biol Cell. 2005;16(11):5141-51. Epub 2005/08/27.

54. Nanes BA, Chiasson-MacKenzie C, Lowery AM, Ishiyama N, Faundez V, Ikura M, et al. p120-catenin binding masks an endocytic signal conserved in classical cadherins. J Cell Biol. 2012;199(2):365-80. Epub 2012/10/17.

55. Anastasiadis PZ, Reynolds AB. Regulation of Rho GTPases by p120-catenin. Curr Opin Cell Biol. 2001;13(5):604-10. Epub 2001/09/07.

56. Noren NK, Liu BP, Burridge K, Kreft B. p120 catenin regulates the actin cytoskeleton via Rho family GTPases. J Cell Biol. 2000;150(3):567-80. Epub 2000/08/10.

57. Korinek V, Barker N, Morin PJ, van Wichen D, de Weger R, Kinzler KW, et al. Constitutive transcriptional activation by a beta-catenin-Tcf complex in APC-/- colon carcinoma. Science. 1997;275(5307):1784-7. Epub 1997/03/21.

58. Morin PJ, Sparks AB, Korinek V, Barker N, Clevers H, Vogelstein B, et al. Activation of beta-catenin-Tcf signaling in colon cancer by mutations in beta-catenin or APC. Science. 1997;275(5307):1787-90. Epub 1997/03/21.

59. Schlegelmilch K, Mohseni M, Kirak O, Pruszak J, Rodriguez JR, Zhou D, et al. Yap1 acts downstream of alpha-catenin to control epidermal proliferation. Cell. 2011;144(5):782-95. Epub 2011/03/08.

60. Silvis MR, Kreger BT, Lien WH, Klezovitch O, Rudakova GM, Camargo FD, et al. alpha-catenin is a tumor suppressor that controls cell accumulation by regulating the localization and activity of the transcriptional coactivator Yap1. Sci Signal. 2011;4(174):ra33. Epub 2011/05/26.

61. Wheelock MJ, Shintani Y, Maeda M, Fukumoto Y, Johnson KR. Cadherin switching. J Cell Sci. 2008;121(Pt 6):727-35. Epub 2008/03/07.

62. Hazan RB, Phillips GR, Qiao RF, Norton L, Aaronson SA. Exogenous expression of N-cadherin in breast cancer cells induces cell migration, invasion, and metastasis. J Cell Biol. 2000;148(4):779-90. Epub 2000/02/23.

63. Nieman MT, Prudoff RS, Johnson KR, Wheelock MJ. N-cadherin promotes motility in human breast cancer cells regardless of their E-cadherin expression. J Cell Biol. 1999;147(3):631-44. Epub 1999/11/05.

64. Utton MA, Eickholt B, Howell FV, Wallis J, Doherty P. Soluble N-cadherin stimulates fibroblast growth factor receptor dependent neurite outgrowth and N-cadherin and the fibroblast growth factor receptor co-cluster in cells. J Neurochem. 2001;76(5):1421-30. Epub 2001/03/10.

65. Williams G, Williams EJ, Doherty P. Dimeric versions of two short N-cadherin binding motifs (HAVDI and INPISG) function as N-cadherin agonists. J Biol Chem. 2002;277(6):4361-7. Epub 2001/12/01.

66. Theisen CS, Wahl JK, 3rd, Johnson KR, Wheelock MJ. NHERF links the N-cadherin/catenin complex to the platelet-derived growth factor receptor to modulate the actin cytoskeleton and regulate cell motility. Mol Biol Cell. 2007;18(4):1220-32. Epub 2007/01/19.

67. Knudsen KA, Sauer C, Johnson KR, Wheelock MJ. Effect of N-cadherin misexpression by the mammary epithelium in mice. J Cell Biochem. 2005;95(6):1093-107. Epub 2005/04/20.

68. Hulit J, Suyama K, Chung S, Keren R, Agiostratidou G, Shan W, et al. N-cadherin signaling potentiates mammary tumor metastasis via enhanced extracellular signal-regulated kinase activation. Cancer Res. 2007;67(7):3106-16. Epub 2007/04/06.

69. Shintani Y, Hollingsworth MA, Wheelock MJ, Johnson KR. Collagen I promotes metastasis in pancreatic cancer by activating c-Jun NH(2)-terminal kinase 1 and up-regulating N-cadherin expression. Cancer Res. 2006;66(24):11745-53. Epub 2006/12/21.

70. Shintani Y, Fukumoto Y, Chaika N, Grandgenett PM, Hollingsworth MA, Wheelock MJ, et al. ADH-1 suppresses N-cadherin-dependent pancreatic cancer progression. Int J Cancer. 2008;122(1):71-7. Epub 2007/08/28.

71. Vogel W, Gish GD, Alves F, Pawson T. The discoidin domain receptor tyrosine kinases are activated by collagen. Mol Cell. 1997;1(1):13-23. Epub 1998/07/11.

72. Vogel W. Discoidin domain receptors: structural relations and functional implications. FASEB J. 1999;13 Suppl:S77-82. Epub 1999/06/03.

73. Alves F, Vogel W, Mossie K, Millauer B, Hofler H, Ullrich A. Distinct structural characteristics of discoidin I subfamily receptor tyrosine kinases and complementary expression in human cancer. Oncogene. 1995;10(3):609-18. Epub 1995/02/02.

74. Leitinger B. Molecular analysis of collagen binding by the human discoidin domain receptors, DDR1 and DDR2. Identification of collagen binding sites in DDR2. J Biol Chem. 2003;278(19):16761-9. Epub 2003/03/04.

75. Abdulhussein R, McFadden C, Fuentes-Prior P, Vogel WF. Exploring the collagen-binding site of the DDR1 tyrosine kinase receptor. J Biol Chem. 2004;279(30):31462-70. Epub 2004/05/12.

76. Carafoli F, Bihan D, Stathopoulos S, Konitsiotis AD, Kvansakul M, Farndale RW, et al. Crystallographic insight into collagen recognition by discoidin domain receptor 2. Structure. 2009;17(12):1573-81. Epub 2009/12/17.

77. Valiathan RR, Marco M, Leitinger B, Kleer CG, Fridman R. Discoidin domain receptor tyrosine kinases: new players in cancer progression. Cancer Metastasis Rev. 2012;31(1-2):295-321. Epub 2012/03/01.

78. Yang G, Li Q, Ren S, Lu X, Fang L, Zhou W, et al. Proteomic, functional and motif-based analysis of C-terminal Src kinase-interacting proteins. Proteomics. 2009;9(21):4944-61. Epub 2009/09/11.

79. Lemeer S, Bluwstein A, Wu Z, Leberfinger J, Muller K, Kramer K, et al. Phosphotyrosine mediated protein interactions of the discoidin domain receptor 1. J Proteomics. 2012;75(12):3465-77. Epub 2011/11/08.

80. Das S, Ongusaha PP, Yang YS, Park JM, Aaronson SA, Lee SW. Discoidin domain receptor 1 receptor tyrosine kinase induces cyclooxygenase-2 and promotes chemoresistance through nuclear factor-kappaB pathway activation. Cancer Res. 2006;66(16):8123-30. Epub 2006/08/17.

81. Shintani Y, Fukumoto Y, Chaika N, Svoboda R, Wheelock MJ, Johnson KR. Collagen I-mediated up-regulation of N-cadherin requires cooperative signals from integrins and discoidin domain receptor 1. J Cell Biol. 2008;180(6):1277-89. Epub 2008/03/26.

82. Dejmek J, Leandersson K, Manjer J, Bjartell A, Emdin SO, Vogel WF, et al. Expression and signaling activity of Wnt-5a/discoidin domain receptor-1 and Syk plays distinct but decisive roles in breast cancer patient survival. Clin Cancer Res. 2005;11(2 Pt 1):520-8. Epub 2005/02/11.

83. Rikova K, Guo A, Zeng Q, Possemato A, Yu J, Haack H, et al. Global survey of phosphotyrosine signaling identifies oncogenic kinases in lung cancer. Cell. 2007;131(6):1190-203. Epub 2007/12/18.

84. Valencia K, Ormazabal C, Zandueta C, Luis-Ravelo D, Anton I, Pajares MJ, et al. Inhibition of collagen receptor discoidin domain receptor-1 (DDR1) reduces cell survival, homing, and colonization in lung cancer bone metastasis. Clin Cancer Res. 2012;18(4):969-80. Epub 2012/01/10.

85. Johnson KR, Lewis JE, Li D, Wahl J, Soler AP, Knudsen KA, et al. P- and E-cadherin are in separate complexes in cells expressing both cadherins. Exp Cell Res. 1993;207(2):252-60. Epub 1993/08/01.

86. Gao M, Duan L, Luo J, Zhang L, Lu X, Zhang Y, et al. Discovery and optimization of 3-(2-(Pyrazolo[1,5-a]pyrimidin-6-yl)ethynyl)benzamides as novel selective and orally bioavailable discoidin domain receptor 1 (DDR1) inhibitors. J Med Chem. 2013;56(8):3281-95. Epub 2013/03/26.

87. Bruns CJ, Harbison MT, Kuniyasu H, Eue I, Fidler IJ. In vivo selection and characterization of metastatic variants from human pancreatic adenocarcinoma by using orthotopic implantation in nude mice. Neoplasia. 1999;1(1):50-62. Epub 2000/08/10.

88. Wahl JK, 3rd, Kim YJ, Cullen JM, Johnson KR, Wheelock MJ. N-cadherin-catenin complexes form prior to cleavage of the proregion and transport to the plasma membrane. J Biol Chem. 2003;278(19):17269-76. Epub 2003/02/27.

89. Grignani F, Kinsella T, Mencarelli A, Valtieri M, Riganelli D, Lanfrancone L, et al. High-efficiency gene transfer and selection of human hematopoietic progenitor cells with a

hybrid EBV/retroviral vector expressing the green fluorescence protein. Cancer Res. 1998;58(1):14-9. Epub 1998/01/13.

90. Maeda M, Johnson KR, Wheelock MJ. Cadherin switching: essential for behavioral but not morphological changes during an epithelium-to-mesenchyme transition. J Cell Sci. 2005;118(Pt 5):873-87. Epub 2005/02/17.

91. Kamohara H, Yamashiro S, Galligan C, Yoshimura T. Discoidin domain receptor 1 isoform-a (DDR1alpha) promotes migration of leukocytes in three-dimensional collagen lattices. FASEB J. 2001;15(14):2724-6. Epub 2001/10/19.

92. Nemoto S, Finkel T. Redox regulation of forkhead proteins through a p66shc-dependent signaling pathway. Science. 2002;295(5564):2450-2. Epub 2002/03/09.

93. Northey JJ, Dong Z, Ngan E, Kaplan A, Hardy WR, Pawson T, et al. Distinct phosphotyrosine-dependent functions of the ShcA adaptor protein are required for transforming growth factor beta (TGFbeta)-induced breast cancer cell migration, invasion, and metastasis. J Biol Chem. 2013;288(7):5210-22. Epub 2013/01/02.

94. Li X, Dy RC, Cance WG, Graves LM, Earp HS. Interactions between two cytoskeleton-associated tyrosine kinases: calcium-dependent tyrosine kinase and focal adhesion tyrosine kinase. J Biol Chem. 1999;274(13):8917-24. Epub 1999/03/20.

95. Faure C, Ramos M, Girault JA. Pyk2 cytonuclear localization: mechanisms and regulation by serine dephosphorylation. Cell Mol Life Sci. 2013;70(1):137-52. Epub 2012/07/18.

96. Sheffield P, Garrard S, Derewenda Z. Overcoming expression and purification problems of RhoGDI using a family of "parallel" expression vectors. Protein Expr Purif. 1999;15(1):34-9. Epub 1999/02/20.

97. Tanaka M, Gupta R, Mayer BJ. Differential inhibition of signaling pathways by dominant-negative SH2/SH3 adapter proteins. Mol Cell Biol. 1995;15(12):6829-37. Epub 1995/12/01.

98. Machida K, Thompson CM, Dierck K, Jablonowski K, Karkkainen S, Liu B, et al. High-throughput phosphotyrosine profiling using SH2 domains. Mol Cell. 2007;26(6):899-915. Epub 2007/06/26.

99. Chen M, She H, Kim A, Woodley DT, Li W. Nckbeta adapter regulates actin polymerization in NIH 3T3 fibroblasts in response to platelet-derived growth factor bb. Mol Cell Biol. 2000;20(21):7867-80. Epub 2000/10/12.

100. Remmers N, Anderson JM, Linde EM, DiMaio DJ, Lazenby AJ, Wandall HH, et al. Aberrant expression of mucin core proteins and o-linked glycans associated with progression of pancreatic cancer. Clin Cancer Res. 2013;19(8):1981-93. Epub 2013/03/01.

101. Shintani Y, Wheelock MJ, Johnson KR. Phosphoinositide-3 kinase-Rac1-c-Jun NH2-terminal kinase signaling mediates collagen I-induced cell scattering and up-regulation of N-cadherin expression in mouse mammary epithelial cells. Mol Biol Cell. 2006;17(7):2963-75. Epub 2006/04/21.

102. Bishop AC, Ubersax JA, Petsch DT, Matheos DP, Gray NS, Blethrow J, et al. A chemical switch for inhibitor-sensitive alleles of any protein kinase. Nature. 2000;407(6802):395-401. Epub 2000/10/03.

103. Shokat K, Velleca M. Novel chemical genetic approaches to the discovery of signal transduction inhibitors. Drug Discov Today. 2002;7(16):872-9. Epub 2003/01/28.

104. Li Y, Lu X, Ren X, Ding K. Small molecule discoidin domain receptor kinase inhibitors and potential medical applications. J Med Chem. 2015;58(8):3287-301. Epub 2015/01/09.

105. Kim HG, Tan L, Weisberg EL, Liu F, Canning P, Choi HG, et al. Discovery of a potent and selective DDR1 receptor tyrosine kinase inhibitor. ACS Chem Biol. 2013;8(10):2145-50. Epub 2013/08/01.

106. Fleming Y, Armstrong CG, Morrice N, Paterson A, Goedert M, Cohen P. Synergistic activation of stress-activated protein kinase 1/c-Jun N-terminal kinase (SAPK1/JNK) isoforms by

mitogen-activated protein kinase kinase 4 (MKK4) and MKK7. Biochem J. 2000;352 Pt 1:145-54. Epub 2000/11/04.

107. Wills MK, Jones N. Teaching an old dogma new tricks: twenty years of Shc adaptor signalling. Biochem J. 2012;447(1):1-16. Epub 2012/09/14.

108. Wills MK, Jones N. Teaching an old dogma new tricks: twenty years of Shc adaptor signalling. Biochem J. 2012;447(1):1-16. Epub 2012/09/14.

109. Vogel W, Gish GD, Alves F, Pawson T. The discoidin domain receptor tyrosine kinases are activated by collagen. Mol Cell. 1997;1(1):13-23. Epub 1998/07/11.

110. van der Geer P, Wiley S, Gish GD, Lai VK, Stephens R, White MF, et al. Identification of residues that control specific binding of the Shc phosphotyrosine-binding domain to phosphotyrosine sites. Proc Natl Acad Sci U S A. 1996;93(3):963-8. Epub 1996/02/06.

111. Migliaccio E, Mele S, Salcini AE, Pelicci G, Lai KM, Superti-Furga G, et al. Opposite effects of the p52shc/p46shc and p66shc splicing isoforms on the EGF receptor-MAP kinase-fos signalling pathway. EMBO J. 1997;16(4):706-16. Epub 1997/02/17.

112. Ahn R, Sabourin V, Ha JR, Cory S, Maric G, Im YK, et al. The ShcA PTB domain functions as a biological sensor of phosphotyrosine signaling during breast cancer progression. Cancer Res. 2013;73(14):4521-32. Epub 2013/05/23.

113. van der Geer P, Wiley S, Gish GD, Pawson T. The Shc adaptor protein is highly phosphorylated at conserved, twin tyrosine residues (Y239/240) that mediate protein-protein interactions. Curr Biol. 1996;6(11):1435-44. Epub 1996/11/01.

114. Smith MJ, Hardy WR, Murphy JM, Jones N, Pawson T. Screening for PTB domain binding partners and ligand specificity using proteome-derived NPXY peptide arrays. Mol Cell Biol. 2006;26(22):8461-74. Epub 2006/09/20.

115. Lev S, Moreno H, Martinez R, Canoll P, Peles E, Musacchio JM, et al. Protein tyrosine kinase PYK2 involved in Ca(2+)-induced regulation of ion channel and MAP kinase functions. Nature. 1995;376(6543):737-45. Epub 1995/08/31.

116. Sasaki H, Nagura K, Ishino M, Tobioka H, Kotani K, Sasaki T. Cloning and characterization of cell adhesion kinase beta, a novel protein-tyrosine kinase of the focal adhesion kinase subfamily. J Biol Chem. 1995;270(36):21206-19. Epub 1995/09/08.

117. Sorokin A, Kozlowski P, Graves L, Philip A. Protein-tyrosine kinase Pyk2 mediates endothelin-induced p38 MAPK activation in glomerular mesangial cells. J Biol Chem. 2001;276(24):21521-8. Epub 2001/03/30.

118. Sanjay A, Houghton A, Neff L, DiDomenico E, Bardelay C, Antoine E, et al. Cbl associates with Pyk2 and Src to regulate Src kinase activity, alpha(v)beta(3) integrin-mediated signaling, cell adhesion, and osteoclast motility. J Cell Biol. 2001;152(1):181-95. Epub 2001/01/10.

119. Lakkakorpi PT, Bett AJ, Lipfert L, Rodan GA, Duong LT. PYK2 autophosphorylation, but not kinase activity, is necessary for adhesion-induced association with c-Src, osteoclast spreading, and bone resorption. J Biol Chem. 2003;278(13):11502-12. Epub 2003/01/07.

120. Zhao M, Finlay D, Zharkikh I, Vuori K. Novel Role of Src in Priming Pyk2 Phosphorylation. PLoS One. 2016;11(2):e0149231. Epub 2016/02/13.

121. Kohno T, Matsuda E, Sasaki H, Sasaki T. Protein-tyrosine kinase CAKbeta/PYK2 is activated by binding Ca2+/calmodulin to FERM F2 alpha2 helix and thus forming its dimer. Biochem J. 2008;410(3):513-23. Epub 2007/11/23.

122. Xiong WC, Macklem M, Parsons JT. Expression and characterization of splice variants of PYK2, a focal adhesion kinase-related protein. J Cell Sci. 1998;111 (Pt 14):1981-91. Epub 1998/07/01.

123. Dikic I, Schlessinger J. Identification of a new Pyk2 isoform implicated in chemokine and antigen receptor signaling. J Biol Chem. 1998;273(23):14301-8. Epub 1998/06/11.

124. Gao M, Duan L, Luo J, Zhang L, Lu X, Zhang Y, et al. Discovery and optimization of 3-(2-(Pyrazolo[1,5-a]pyrimidin-6-yl)ethynyl)benzamides as novel selective and orally bioavailable

discoidin domain receptor 1 (DDR1) inhibitors. J Med Chem. 2013;56(8):3281-95. Epub 2013/03/26.

125. Valencia K, Ormazabal C, Zandueta C, Luis-Ravelo D, Anton I, Pajares MJ, et al. Inhibition of collagen receptor discoidin domain receptor-1 (DDR1) reduces cell survival, homing, and colonization in lung cancer bone metastasis. Clin Cancer Res. 2012;18(4):969-80. Epub 2012/01/10.

126. Ambrogio C, Gomez-Lopez G, Falcone M, Vidal A, Nadal E, Crosetto N, et al. Combined inhibition of DDR1 and Notch signaling is a therapeutic strategy for KRAS-driven lung adenocarcinoma. Nat Med. 2016;22(3):270-7. Epub 2016/02/09.

127. Ali-Rahmani F, FitzGerald DJ, Martin S, Patel P, Prunotto M, Ormanoglu P, et al. Anticancer Effects of Mesothelin-Targeted Immunotoxin Therapy Are Regulated by Tyrosine Kinase DDR1. Cancer Res. 2016;76(6):1560-8. Epub 2016/01/01.

128. Aguilera KY, Rivera LB, Hur H, Carbon JG, Toombs JE, Goldstein CD, et al. Collagen signaling enhances tumor progression after anti-VEGF therapy in a murine model of pancreatic ductal adenocarcinoma. Cancer Res. 2014;74(4):1032-44. Epub 2013/12/19.

129. Aguilera KY, Goldstein CD, Rivera LB, Bradshaw AD, Ding K, Brekken RA. SPARC as a regulator of collagen signaling in pancreatic cancer. Cancer Res. 2014;74(182).

130. Hingorani SR, Wang L, Multani AS, Combs C, Deramaudt TB, Hruban RH, et al. Trp53R172H and KrasG12D cooperate to promote chromosomal instability and widely metastatic pancreatic ductal adenocarcinoma in mice. Cancer Cell. 2005;7(5):469-83. Epub 2005/05/17.

131. Okigaki M, Davis C, Falasca M, Harroch S, Felsenfeld DP, Sheetz MP, et al. Pyk2 regulates multiple signaling events crucial for macrophage morphology and migration. Proc Natl Acad Sci U S A. 2003;100(19):10740-5. Epub 2003/09/10.

132. Ilic D, Furuta Y, Kanazawa S, Takeda N, Sobue K, Nakatsuji N, et al. Reduced cell motility and enhanced focal adhesion contact formation in cells from FAK-deficient mice. Nature. 1995;377(6549):539-44. Epub 1995/10/12.

133. Bhattacharya SK, Aspnes GE, Bagley SW, Boehm M, Brosius AD, Buckbinder L, et al. Identification of novel series of pyrazole and indole-urea based DFG-out PYK2 inhibitors. Bioorg Med Chem Lett. 2012;22(24):7523-9. Epub 2012/11/17.

134. Alexandropoulos K, Cheng G, Baltimore D. Proline-rich sequences that bind to Src homology 3 domains with individual specificities. Proc Natl Acad Sci U S A. 1995;92(8):3110-4. Epub 1995/04/11.

135. Saksela K, Permi P. SH3 domain ligand binding: What's the consensus and where's the specificity? FEBS Lett. 2012;586(17):2609-14. Epub 2012/06/20.